Science of the Total Environment 806 (2022) 150206

Contents lists available at ScienceDirect

Science of the Total Environment

journal homepage: www.elsevier.com/locate/scitotenv

Hydrochemical characterization, spatial distribution, and geochemical controls on arsenic and boron in waters from arid Arica and Parinacota, northern Chile

G.P. Pincetti-Zúniga [a,*], L.A. Richards [a,*], L. Daniele [b,c], A.J. Boyce [d], D.A. Polya [a]

[a] Department of Earth and Environmental Sciences and Williamson Research Centre for Molecular Environmental Science, University of Manchester, Manchester M13 9PL, UK
[b] Departamento de Geología, Facultad de Ciencias Físicas y Matemáticas, Universidad de Chile, Santiago, Chile
[c] Centro de Excelencia en Geotermia de Los Andes (CEGA), Facultad de Ciencias Físicas y Matemáticas, Universidad de Chile, Santiago, Chile
[d] Scottish Universities Environmental Research Centre, East Kilbride G75 0QF, UK

HIGHLIGHTS

- Regional hydrochemical characterization of 90 water samples in 5 basins
- Arsenic >10 μg/L in 72% overall and in 44% of samples used for drinking (n = 32)
- Compilation of ~1500 points suggests regional water quality issues (As, B, Cd, Pb)
- Stable H and O isotopes show freshwater mixed with thermal and evaporated sources
- Type of geothermal source determines fate of As downstream: acid-SO_4 vs neutral-Cl

GRAPHICAL ABSTRACT

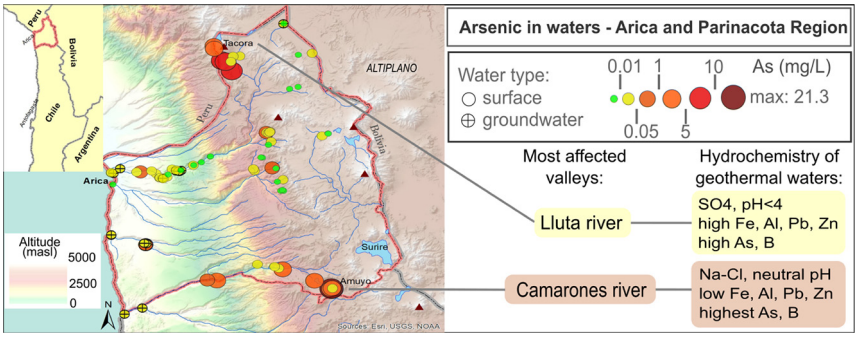

ARTICLE INFO

Article history:
Received 23 June 2021
Received in revised form 18 August 2021
Accepted 3 September 2021
Available online 8 September 2021

Editor: José Virgílio Cruz

Keywords:
Northern Chile
Water quality
Hydrochemical evolution
Arsenic
Boron
Geothermal waters

ABSTRACT

The livelihood of inhabitants from rural agricultural valleys in the arid Arica and Parinacota Region, northernmost Chile, strongly depends on water from high altitude rainfall and runoff to lower elevation areas. However, elevated arsenic, boron, and other potentially harmful elements compromise water quality, especially in rural areas. Samples (n = 90) of surface, underground, cold, geothermal springs, and treated and raw tap water were studied to assess water quality and to determine the main geochemical controls on water composition, origin, and geochemical evolution along dominant flowpaths. Water from major river basins across the region (Lluta, San Jose, Codpa-Chaca, Camarones and Altiplanicas) were collected for hydrogeochemical analysis of a suite of major and trace elements, δD and $\delta^{18}O$. Our new dataset was supplemented by hydrochemical data (n > 1500 data points) from secondary sources. Results show that 72% of the collected samples had As >10 μg/L (WHO drinking water provisional guideline) and affected 44% of the studied waters used for drinking (n = 32). Based on Chilean irrigation guidelines, elevated salinity (EC > 0.75 mS/cm) affected 80% of sampled waters, which were also impacted by high B (89% > 0.75 mg/L), and As (31% > 50 μg/L). Water composition was strongly controlled by geothermal water and freshwater mixing in high altitude areas. Magnitude and fate of As and B concentration was determined by the geothermal input type. Highest As (~21 mg/L) was associated with circum-neutral Na-Cl waters in Camarones basin, while lower As (~5 mg/L) with acid SO_4 waters in Lluta basin. Additionally, evaporative concentration and sediment-water interactions were shown to control the

* Corresponding authors.
E-mail addresses: gianfranco.pincetti@gmail.com (G.P. Pincetti-Zúniga), laura.richards@manchester.ac.uk (L.A. Richards).

https://doi.org/10.1016/j.scitotenv.2021.150206
0048-9697/

level of As in surface and groundwaters downstream. This works provides a comprehensive analysis and a conceptual model of geochemical controls on regional water compositions, contributing to better understanding the geochemical processes underpinning the water quality challenges in northern Chile.

1. Introduction

Arica and Parinacota (hereafter A&P) is the northernmost region of Chile, located 2000 km north of Santiago and encompassed within the Atacama Desert, the driest in the world (Clarke, 2006; Rech et al., 2010). The scarce freshwater sources from this region, including surface and groundwaters, are often characterized by slight to moderate salinity, and in many cases, by high concentrations of arsenic (As), boron (B), and other potentially toxic elements (Torres and Acevedo, 2008; Bundschuh et al., 2012; Leiva et al., 2014; Rámila et al., 2015; Guerra et al., 2016; Tapia et al., 2018, 2019; Morales-Simfors et al., 2020). The occurrence of elevated As, especially in water sources used for drinking, is a worldwide problem that potentially affects the health of millions of people chronically exposed to concentrations exceeding 10 μg/L (Bhattacharya et al., 2002; Smedley and Kinniburgh, 2002; Ravenscroft et al., 2009; Bundschuh et al., 2012; Polya and Lawson, 2015; Khan et al., 2020), which is the current provisional guideline by the World Health Organization (WHO, 2017) and the Chilean permissible limit (INN, 2006). The rural population in A&P is estimated to be ~19,000 inhabitants (INE, 2018), of which many, especially indigenous people from remote Aymara communities, do not have access to a safe drinking water source (Sancha and O'Ryan, 2008).

The occurrence of elevated As in water, soils, and air, is a major environmental issue in parts of northern Chile (Hopenhayn-Rich et al., 2000; Caceres et al., 2005; Sancha and O'Ryan, 2008; Arriaza et al., 2018). Many studies have identified a high prevalence of bronchopulmonary disease, lung and bladder cancer, hypertension, diabetes, and increased child mortality (Ferreccio et al., 2000; Hopenhayn-Rich et al., 2000; Smith et al., 2000; Sancha and O'Ryan, 2008; Steinmaus et al., 2013) in people exposed to high As (~ 800 μg/L) in drinking water, notably in Antofagasta city, which is located some 700 km to the south of A&P (Borgono et al., 1977; Smith et al., 1992, 2017; Steinmaus et al., 2016). In Arica city, the capital of A&P, the concentration of As in drinking water has long been reported to be <10 μg/L (Steinmaus et al., 2013). However, in rural areas in A&P, the concentration of As in natural waters potentially used for drinking and irrigation are often much greater (Mahan et al., 2020), especially in the Camarones river where concentrations of As are generally >1 mg/L (Cornejo et al., 2004, 2008). Efforts have accordingly been made for developing low-cost remediation techniques (M.G. García et al., 2004; Cornejo et al., 2008; Bundschuh et al., 2012; Litter et al., 2012; McClintock et al., 2012). Moreover, high concentrations of As have been found in hair and tissues collected in mummies from the Chinchorro pre-Columbian culture, which thrived in A&P valleys and coastal areas over 7000 years ago (Byrne et al., 2009; Arriaza et al., 2010, 2018), providing evidence of ancient long-term exposure to extremely high As in local populations within this region.

The occurrence of elevated As, B, and other potentially harmful elements in northern Chile is generally associated with geological features such as the regional tectonic framework of subduction (Moreno and Gibbons, 2007; García et al., 2017; Mukherjee et al., 2019), recent Andean volcanism and leaching of volcanic rocks (Tapia et al., 2019, 2021; Morales-Simfors et al., 2020), geothermal activity (Webster and Nordstrom, 2003; López et al., 2012; Tapia et al., 2019, 2021), and high evaporation rates and slow flushing of high-As sediments, as associated with the hyper-aridity of the Atacama Desert (Clarke, 2006; Rissmann et al., 2015). In some cases, elevated concentrations of As are directly linked to the input of hot geothermal fluids or the dissolution of As-bearing minerals found in volcanic rocks, which are abundant in the headwaters of Andean river basins (Romero et al., 2003; Webster and Nordstrom, 2003; Tassi et al., 2010; Capaccioni et al., 2011; Risacher et al., 2011; López et al., 2012; Guerra et al., 2016; Tapia et al., 2018, 2019, 2021). Additionally, this region is well known for the abundance of hydrothermal alteration zones and associated ore deposits, especially of sulphur, copper, silver, gold, and borates (Ferraris and Vila, 1990; García et al., 2017; Tapia et al., 2018; Murray et al., 2019). The exploitation of these and other mineral resources can contribute additional dissolved substances into water sources, or can potentially lead to increased weathering of As-bearing rocks (Pizarro et al., 2010; Allende et al., 2014).

Studies have also evidenced accumulation of metals and metalloids in the sediments in A&P (Valenzuela et al., 2009; Baeza et al., 2015; Copaja et al., 2018), which can potentially affect surface and groundwater quality if mobilized. Further, elevated salinity and high concentrations of As and B affect the water quality and possible uses of agricultural land (Hem, 1985; Torres and Acevedo, 2008), especially in the Lluta and Camarones valleys (Cornejo et al., 2004; Torres and Acevedo, 2008). In many cases, surface water can only be used for the irrigation of salinity-resistant crops such as corn and onions (Torres and Acevedo, 2008; Cornejo-Ponce and Acarapi-Cartes, 2011).

Despite previous studies covering aspects of water quality in A&P, there is a lack of an integrated view of the main hydrogeological controls and the relative importance of the various geochemical processes impacting the chemical composition of natural waters within the main basins (i.e. Lluta, San Jose, Camarones, and Altiplanicas basins) in A&P. In general, the water quality issues observed in natural waters in A&P are assumed to be volcanic-related (López et al., 2012; Tapia et al., 2019; Morales-Simfors et al., 2020), although the potential variability in the sources of natural pollution, especially the differences in geothermal inputs, remains inadequately considered. Additionally, to date there has been no detailed characterization of the geochemical variations in waters from different sources, notably surface water, groundwater, cold springs, and thermal springs.

This study aims to assess and compare the hydrochemistry and geochemical processes impacting the quality of water sources used for drinking and irrigation in A&P, with a primary focus on As and B due to their potential implications on public health and agriculture, respectively. We hypothesize that the magnitude and distribution of geogenic contaminants strongly depends on altitude variations and the relative contribution of solutes from geothermal/mineralised areas. This study's objectives are to (i) geochemically characterise various water sources in carefully selected rural areas across the dominant basins within A&P, including where data remains underrepresented; (ii) comprehensively compile available secondary geochemical data, including government public reports and peer-reviewed publications; (iii) interpret the variability of water quality and dominant geochemical processes among the studied river basins (valleys) and water sources, (iv) propose a conceptual model identifying the relative importance and spatial distribution of the main geochemical mechanisms controlling the hydrochemistry in A&P.

2. Study area

A&P region (17° 30' to 19° 13′ S, 68° 54' to 70° 22′ W) is the northernmost administrative division of Chile, bordering Peru to the north and Bolivia to the east (Fig. 1A). The main geographical features of this region are largely distributed in N-S belts, including from west to east: Coastal Cordillera, Central Depression valleys and pampas, Pre-

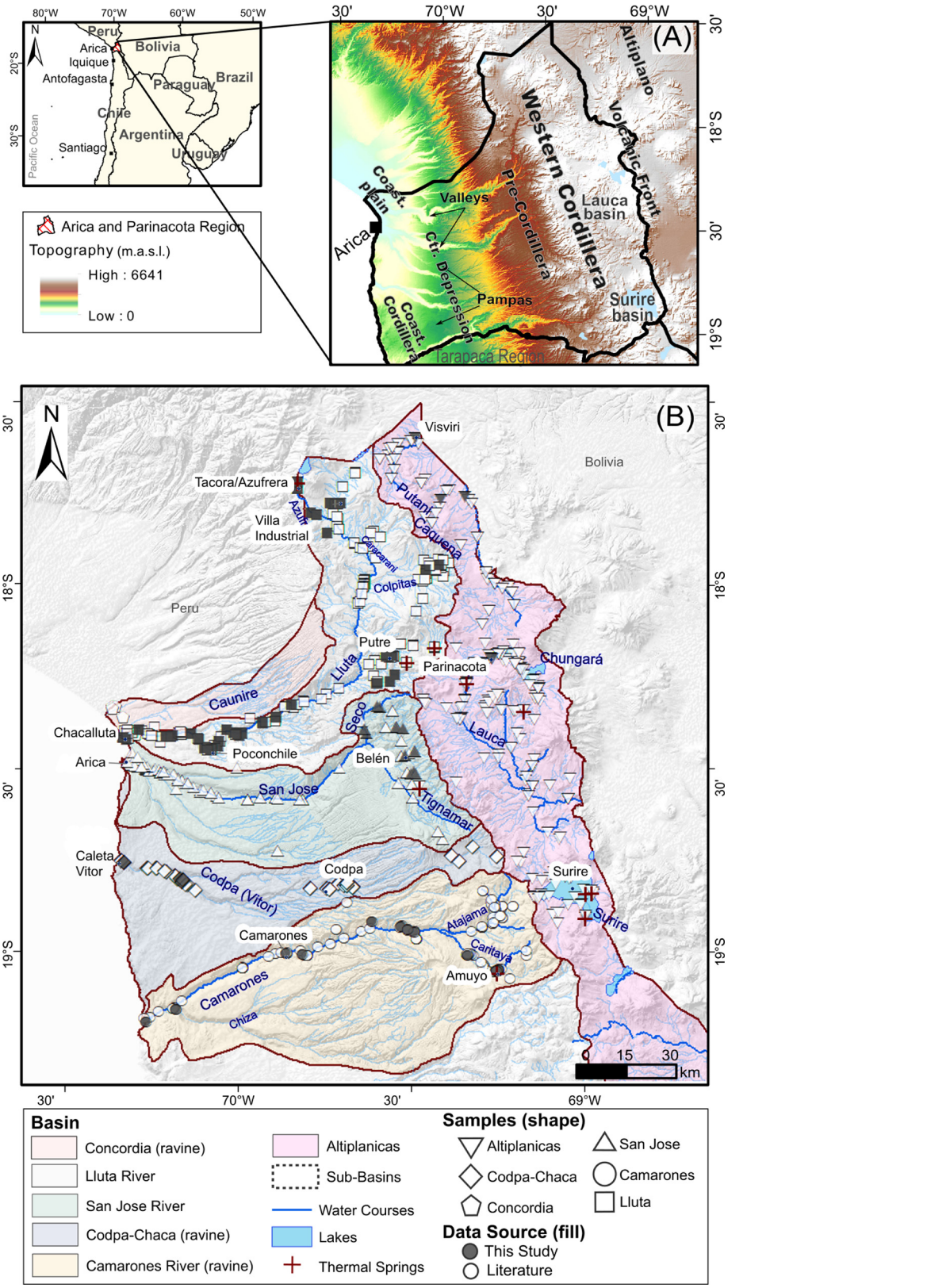

Fig. 1. (A) Location of the Arica and Parinacota region and topographic regional map which indicates the main geomorphological units (B) Map showing the main hydrological features and watersheds. This map shows the main rivers, thermal waters, and the location of water samples considered in this study (both from this study in filled symbols and from other sources in open symbols, notably Japan International Cooperation Agency (JICA), 1995; Arrau, 1997; Risacher et al., 1999, 2011; SEA-ESSAT, 1999; SEA-SRK Consulting, 2002; Herrera et al., 2006; SEA-SMI, 2008; DGA-DICTUC, 2008; SEA-SGA, 2010; UTA, 2010; SEA-GHD, 2011; DOH-R&Q ingeniería, 2012; DGA-Mayco, 2013; SEA-Energia Andina, 2013; DGA-Arrau Ingeniería, 2013; CNR-GeoHidrologia Consultores, 2014; INH, 2014; DGA-AMEC, 2014; DGA-Matraz Consultores, 2015; DGA-Con Potencial Consultores, 2016; DGA-ICASS, 2016; Cornejo et al., 2019; DGA, 2020).

Cordillera foothills, western Cordillera and active volcanic front, and parts of the Altiplano highland (Fig. 1A). Six watersheds are encompassed within this region (from north to south): Concordia ravine, Lluta river, San Jose river (Azapa valley), Codpa river (Chaca valley), Camarones river, and Altiplanicas (Fig. 1B). From these, only Lluta is a perennial stream that reaches the sea all year round.

The climate of A&P is mostly arid as it is within the Atacama Desert (Clarke, 2006), although there are geographical differences across the region especially due to changes in altitude and distance to the sea (Sarricolea et al., 2017). In coastal and lower sections (<2000 m.a.s.l.) of the valleys and pampas, the annual rainfall is typically negligible (Houston and Hartley, 2003; Clarke, 2006). In contrast, annual rainfall is often >350 mm in areas >3000 m.a.s.l (Sarricolea et al., 2017), mostly associated with the annual *Altiplanic winter* or South American Summer Monsoon, typically between January and March (Houston and Hartley, 2003; Marengo et al., 2012). The main rivers within the A&P region are of pluvial and nival regime, hence their average volume of discharge depends on rainfall during the summer months. In terms of water availability and economic uses, the most important rivers are the San Jose (ephemeral stream), Lluta (perennial stream), Codpa (ephemeral stream), and Camarones (ephemeral stream) (Fig. 1B).

2.1. Geological setting

Chile is located above a subduction zone formed by the convergence of the Nazca and the South American Plates. This constitutes the primary control on the regional geology (Moreno and Gibbons, 2007). The subduction process causes the deformation, lifting, thickening of the continental crust, as well as calc-alkaline volcanism (Moreno and Gibbons, 2007; M. García et al., 2017), leading to contrasting geographical conditions (Fig. 1A). The local geology comprises mostly volcanic and volcano-sedimentary sequences (Fig. 2A), including rocks spanning from the Precambrian era to the Holocene, with younger rocks generally found towards the east, where the current volcanic arc is located (M. García et al., 2004; Servicio Nacional de Geología y Minería, 2012; García et al., 2017). The lithological units in this region are broadly

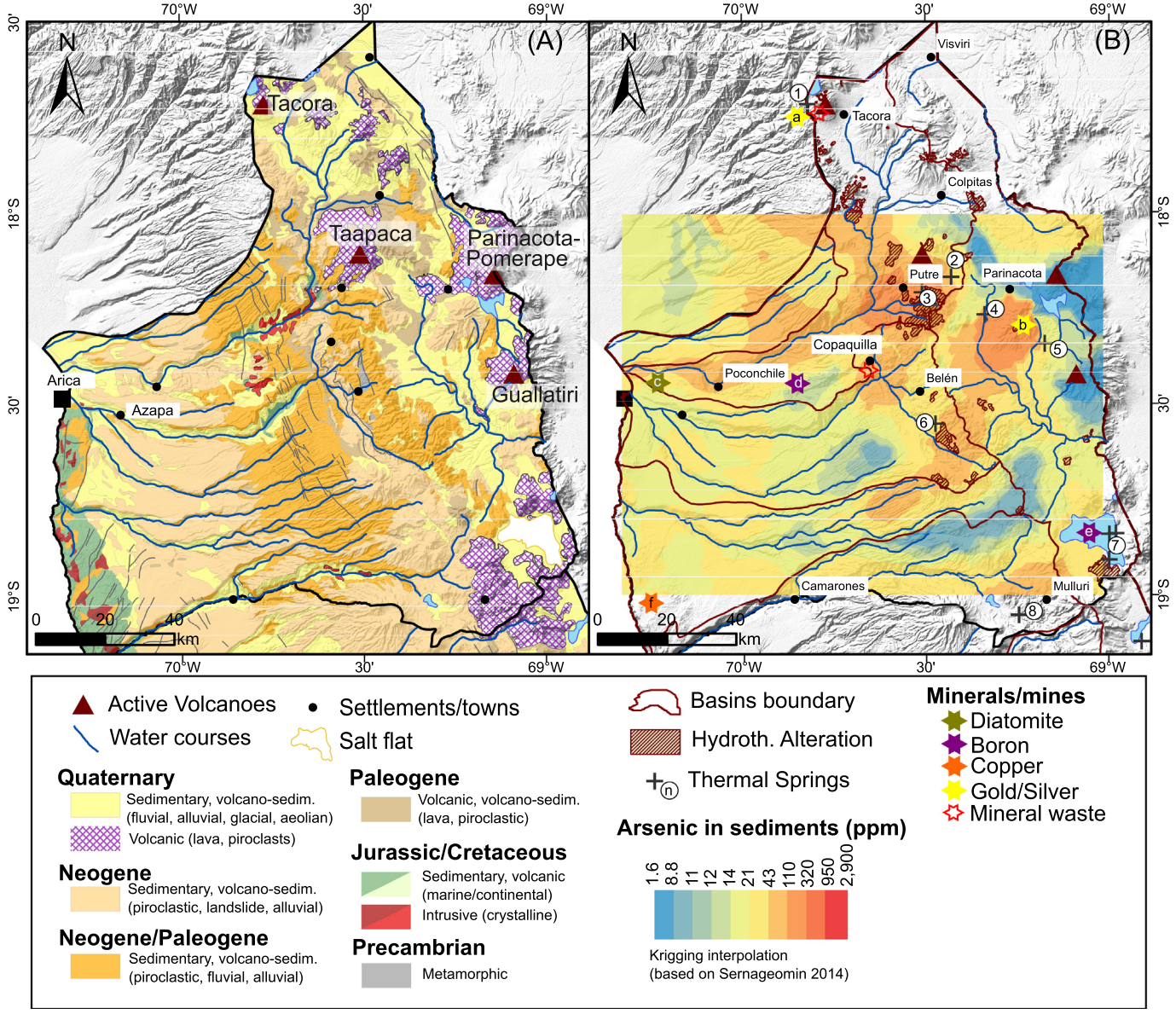

Fig. 2. (A) Simplified geological map of the Arica and Parinacota region (based on geological map 1:1,000,000 Sernageomin, 2003; García et al., 2004) (B) Map illustrating the geochemical anomaly of As in sediments (ppm) by Kriging interpolation (ArcGIS) in a quadrant within the study area (based on data from sediments collected by Sernageomin (Baeza et al., 2015, Lacassie et al., 2014). Relevant locations in the map (by numbers and letters): Thermal springs: 1. Tacora/Aguas Calientes 2. Las Cuevas 3. Jurase 4. Pozo Lauca 5. Chirigualla 6. Chitune 7. Surire-Polloquere 8. Amuyo. Minerals/Mines: a. Pucamarca (Peru) b. Choquelimpie c. Imerys (exCelite) d. Quiborax e. Quiborax-Surire f. Pampa Camarones.

distributed in N-NW/S-SE bands (Fig. 2A), from west to east: (i) the Jurassic/Cretaceous volcanic arc and marine/continental back-arc at the coast and forming Coastal Cordillera, (ii) Paleogene to Neogene volcano-sedimentary rocks at the Central Depression and Pre Cordillera, (iii) Quaternary volcanic deposits associated with the active volcanic front within the Central Andean Volcanic Zone (CAVZ) which includes Tacora, Taapaca, Parinacota-Pomerape, and Guallatiri active volcanoes (Fig. 2A) (Moreno and Gibbons, 2007; Tassi et al., 2010; Capaccioni et al., 2011; Inostroza et al., 2020); and (iv) Quaternary volcanic rocks and sedimentary deposits covering valleys and overlaying older rocks throughout the region (Sernageomin, 2003; Moreno and Gibbons, 2007).

Many geothermal springs (Fig. 2B) and hydrothermal alteration/mineralization zones are found in A&P, often associated with recent and current andesitic to dacitic volcanic activity (Risacher et al., 2003, 2011; Tassi et al., 2010; Capaccioni et al., 2011; Lagos Durán, 2016; Cornejo et al., 2019; Inostroza et al., 2020). These geothermal sites are a major source of high solute concentrations in local water systems. Additionally, important sources of solutes are derived from hydrothermal alteration zones and mineral deposits (Fig. 2B), notably of copper, gold, silver, lithium, and boron deposits (e.g. notable active mines: Choquelimpie-gold, Pampa Camarones-copper, Quiborax-borates) (Fig. 2B). Suggestions of an important Paleocene to early Oligocene porphyry-Cu-Mo belt have been made (García et al., 2017), while high-sulfidation epithermal Au-Ag mineralization areas of Miocene to early Pliocene age constitute a metallogenic belt of current economic interest in Chile and Peru (García et al., 2017 and references therein). However, to date, no large ore deposits have been found in A&P and only a few mines are currently operating (Fig. 2B) but the interest in mineral exploration in this region is increasing (Tapia, 2019). Mineralised and hydrothermal alteration areas at the headwaters of river systems in A&P are often relevant to water quality downstream, notably at the Lluta basin where abandoned sulphur-extraction waste from such deposits causes impact on water quality to tributaries and lower sections of the Lluta river (Leiva et al., 2014; Guerra et al., 2016).

Studies on the composition of Quaternary sediments (fraction <180 μm) of the main rivers within the region have shown a geochemical anomaly of As (Fig. 2B), and other elements such as Zn and Pb, forming the Putre-Camina N-NW regional anomaly in the Western Cordillera (Lacassie et al., 2014; Baeza et al., 2015). Sediments rich in As are mostly accumulated in alluvial and fluvial deposits, especially in the Lluta (max 700 μg/g As), Lauca (578 μg/g As), and Camarones (75 μg/g As) rivers deposits (Fig. 2B) (Baeza et al., 2015).

2.2. Hydrogeological setting

The main hydrological features (Fig. 1B) include exorheic river basins (Lluta, Camarones, San Jose, Codpa-Chaca), and endorheic basins at higher altitudes (Lauca, Surire, Caquena-Putani). The main drainage system is the Lluta river basin with a catchment area of 3500 km^2 and river extension of 150 km. Most of the aquifers studied in this region are enclosed in the narrow valleys with greater vertical and horizontal development near coastal areas – examples include the Lluta and Azapa aquifers. These units are mostly comprised of layers of medium to coarse grain weathered volcanic material, and usually are of limited extension (<5 km) and depth (<100 m) (DGA-ICASS, 2016).

3. Methods

3.1. Water sampling and analytical procedures

The collection of 90 water samples from different types of sources took place during April 2018 (Fig. 1B), including: (i) surface waters (SW, $n = 30$) taken directly from natural streams and irrigation canals; (ii) groundwaters from dug wells and tube wells (GW, $n = 15$), and from cold springs (CS, $n = 25$); (iii) tap (T, $n = 14$), including treated (t) and untreated (u) water used for drinking; and (iv) thermal springs (TS, $n = 6$). The samples were selected on consideration of accessibility, relevance for drinking and agriculture, and/or hypothesized impact of the waters on the hydrochemistry of the studied river systems (especially Lluta and Camarones river basins). The number of samples per river basin in decreasing order was: Lluta ($n = 47$), Camarones ($n = 18$), San Jose ($n = 12$), Altiplanicas ($n = 8$), and Codpa-Chaca ($n = 5$). Not all types of water were collected from all basins studied due to accessibility and time constraints (e.g. in Codpa-Chaca only GW samples were collected).

Sampling methods were broadly based on protocols described elsewhere (Polya and Watts, 2017; Richards et al., 2017). In-situ physicochemical parameters measurements, including pH, oxidation-reduction potential (ORP – Ag/AgCl electrode), temperature, and electrical conductivity (EC), were made in-situ using a portable multimeter (Hach - HQ40D). Total As was estimated in-situ using a ITS Econo-Quick As kit (Part number: 481298). Alkalinity was measured using a field test kit (Merck MColortest 1,111,090,001).

Upon sampling, waters for major, minor, and trace anion and cation analyses were filtered (0.45 μm regenerated cellulose syringe filters, Minisart RC25 17,765-K) and collected in 100 mL Schott glass bottles, which had previously been acid-washed in 10% HNO_3. Sub-samples for cation analyses were preserved by the addition of 1 mL of 5 M HNO_3 to pH < 2. The preservation pH was verified in-situ with pH test strips (Merck – SupelcopH; part number 109535). In addition, sub-samples for analyses of As speciation were collected using pre-conditioned solid-phase extraction (SPE) cartridges (Agilent, part numbers 12162040B, 12162044B) (Watts et al., 2010). Sub-samples for stable isotope analysis (δ^2H and $\delta^{18}O$) were directly collected in 60 mL amber glass bottles. All the samples were kept at a cool temperature (4 °C) prior to analysis.

Chemical analyses to determine major and trace elements composition were performed at the Manchester Geochemistry Analytical Unit (MAGU), using: (i) ICP-AES (Perkin-Elmer Optima 5300) to determine Ca, Na, Mg, K, Si, Mn, Al, Fe, P, Ba, B, Li, and S; the latter measured individually to avoid interferences, (ii) ICP-MS (Agilent 7700) for As, Cr, Cu, Pb, Mn, Ni, Se, Sr, V, and Zn, (iii) Ion Chromatography (IC, Dionex ICS5000) to determine Cl, SO_4, NO_3, NO_2, F, Br, and PO_4, (iv) HPLC-MS (Agilent 6130) for As speciation in a sub-set of samples >10 μg/L ($n = 72$), and (v) total carbon (TC) and total inorganic carbon (TIC) (Shimadzu TOC-V CPN analyser). Many samples were slightly to moderately saline and prior to chemical analyses, with dilutions up to a factor of 100 times needed to 0.1% salinity to minimise matrix effects (Todolí et al., 2002). Additionally, stable isotope analysis (δ^2H and $\delta^{18}O$) was conducted at the Scottish Universities Environmental Research Centre (East Kilbride) using a Thermo Scientific Delta V mass spectrometer. Water stable isotope data are reported as per mil (‰) variations from the V-SMOW (Standard Mean Ocean Water) standard.

3.2. Data quality control and assurance (QA/QC)

A series of quality control and quality assurance procedures were implemented, broadly following methods indicated elsewhere (Polya and Watts, 2017; Richards et al., 2017; Pincetti-Zúniga et al., 2020). Major and trace elements were measured in duplicate in at least 10% of the samples to assess the precision of the results (for duplicates mean values are reported). To determine accuracy, several calibration standard measurements were considered, including: (i) ICP-MS: six-point calibration at 0, 1, 5, 10, 50, and 100 μg/L;(ii) ICP-AES: 8 point calibration at 0, 0.01, 0.05, 0.1, 1, 5, 10, 20, and 100 mg/L; (iii) IC: 5 point calibration at 0, 0.2, 1, 5, 20 mg/L for Cl, SO_4, NO_3; and 0, 0.02, 0.1, 0.5, 2 mg/L for F; and (iv) TC: 4 calibration points at 0, 1, 5 20 mg/L. Preliminary results from ICP-MS and ICP-AES were subject to a calibration model using a weighted least-squares linear regression (Miller, 1991; Polya and Watts, 2017). Certified reference materials (CRM), including CRMs SPS-SW1, CA011c, and 1640a for major and trace cations,

and LGC6020 for anions, were used to validate the results. Detection limits were estimated using the mean standard deviation of blank measurements. The reproducibility of the stable isotopes (δ^2H and $\delta^{18}O$) data was based on within-run repeat analyses of at least three standard waters.

The chemical composition results were subject to charge balance error calculations (CBE) made using milliequivalent concentrations of major elements, normatively considered as Ca^{2+}, Mg^{2+}, Na^{+}, K^{+}, Cl^{+}, SO_4^{2-}, NO_3^-, HCO_3^-, Br^-, Al^{3+}, Fe^{2+}, and Mn^{2+}. In the case of naturally acidic samples with pH <2, concentrations of H^+ were included in charge balance calculations. Further, calculated total dissolved solids (TDS) were estimated based on the chemical analysis results and were compared to in-situ EC.

3.3. Existing hydrochemical data compilation and processing

An extensive review and compilation of secondary hydrochemical data from A&P was conducted. Numerous open-access studies and reports mostly commissioned by the National Water Resources Agency (*Dirección General de Aguas;* DGA), through external and/or private consultants, were reviewed (Japan International Cooperation Agency (JICA), 1995; Arrau, 1997; Risacher et al., 1999, 2011, SEA-ESSAT, 1999; SEA-SRK Consulting, 2002; Herrera et al., 2006; SEA-SMI, 2008; DGA-DICTUC, 2008; SEA-SGA, 2010; UTA, 2010; SEA-GHD, 2011; DOH-R&Q ingeniería, 2012; DGA-Mayco, 2013; SEA-Energia Andina, 2013; DGA-Arrau Ingeniería, 2013; CNR-GeoHidrologia Consultores, 2014; INH, 2014; DGA-AMEC, 2014; DGA-Matraz Consultores, 2015; DGA-Con Potencial Consultores, 2016; DGA-ICASS, 2016; Cornejo et al., 2019; DGA, 2020); many of these focused on water availability and agricultural water management. Hydrochemical characterization was not always included in the reports or was often incomplete or inconsistent. In addition, water quality records (including 33 monitoring stations with historical or recent data; from which 16 are currently operating) available from the DGA website (DGA, 2020) were retrieved. The materials reviewed included 25 reports containing hydrochemical records, from which 22 were government-financed projects and 3 were peer-reviewed publications. The collected records contained 2217 hydrochemical data points, which included surface and underground sources from all six basins within A&P. The collected data were checked for consistency of parameters, missing values, and outliers (based on linear regression of parameters vs Cl). The dataset was reduced to 1503 points meeting the criteria of (i) inclusion of all major elements (Na, Ca, Mg, K, Cl, SO_4, HCO_3) and (ii) a CBE <20%. Further filtering was applied to consider data which included As concentrations (1249 samples).

3.4. Statistical methods and data visualization

Data processing, statistical analysis, and graphics were performed using Origin v2017 software (Oracle). For statistical purposes, parameters with values below the detection limit (BDL) were replaced by half the detection limit value (Farnham et al., 2002). Analytes with missing values and/or BDL in >15% of the samples were excluded from multivariate statistical analysis only to optimise results (based on Farnham et al., 2002). Statistical tools used included Shapiro-Wilk normality test, linear correlations, principal component analysis (PCA) and hierarchical cluster analysis (HCA) by Ward's method (Euclidian distances by correlation) (Vega et al., 1998). Treated tap waters samples ($n = 6$) were excluded from statistical analysis of geochemical processes. Selected chemical (Na, K, Ca, Mg, Cl, SO_4, HCO_3, Si, B, and As) and physicochemical parameters (pH, EC) were used for multivariate statistical analysis. For the application of the multivariate methods, a logarithmic transformation of the data and normalization (by TDS) was implemented for visualization and interpretation (Vega et al., 1998).

Mapping and spatial analysis were made with ArcGIS 10.2.2, using DEM and service layers from several sources, including Earth Explorer (USGS, 2021), Open Street Map (OSMF, 2019), DIVA-GIS (2020), and IDE-geoportal Chile (Ministerio de Bienes Nacionales, 2019). The Geochemist's Work Bench software and Thermo database were used for graphics, geochemical modelling, TDS calculation, and saturation indices (SI = log[IAP/Ksp]).

4. Results

4.1. QA/QC results

Major cations (Ca, Na, Mg, and K) CRMs results were within ±10% with respect to the certified reference values, while minor cations such as Fe, Al, and Mn were generally within ±15%, with increasing deviation close to their respective detection limit. Most of the analytes (ICPMS: As, Ba, Cr, Mn, Pb, V, and Zn; IC: Cl, SO_4, NO_3, and F) had <± 10% difference with respect to the relevant CRM. Most samples ($n = 88$) had a CBE within ±10%, except for 2 samples with CBE between ±10% and ± 15%. A comparison of TDS and Cl resulted in a strong linear fit ($R^2 = 0.96$). A Shapiro-Wilk normality test and the observation of Q-Q plots and histograms resulted in the rejection of normality for all hydrochemical analytes.

4.2. Hydrochemistry of waters collected in this study

4.2.1. In-situ physicochemical parameters

The studied waters showed a great variability in in-situ physicochemical parameters, especially pH (range 1.5–9.6; median 7.3) and EC (range 0.1–20 mS/cm; median 2 mS/cm) depending on the source type and geographical location (Table 1S and Table 2S in Supplementary Materials). The most acidic samples (pH < 2) correspond to surface waters located near Tacora and associated with TS, whereas the maximum pH values were measured in groundwaters associated with CS samples. The lowest EC values correspond to CS waters from high ground areas typically >2500 m.a.s.l.; whereas TS and SW had the highest values reaching a maximum of ~20 mS/cm nearby Tacora/Aguas Calientes thermal springs (Lluta basin), followed by Amuyo springs (Camarones basin) (Fig. 1B). The studied waters were mostly oxidising, with ORP values generally >100 mV (median ORP 197 mV Ag/AgCl).

4.2.2. Major cations and anions

The cationic composition showed the greatest variability among different locations, especially between Lluta and Camarones valleys waters. Major constituents were dominated by Na (range 5 - 1920 mg/L; median 234 mg/L), followed by Ca (range 1 - 700 mg/L; median 110 mg/L), Mg (range 0.2 - 180 mg/L; median 22 mg/L), and K (range 0.4 - 250; median 16 mg/L). The maximum Na concentrations occurred in geothermal waters from Amuyo thermal springs in the Camarones valley, whereas the highest concentrations of Ca, Mg, and K (950, 290, and 150 mg/L, respectively) were found in the Lluta valley. The anionic components were dominated by Cl (range 1 - 4300 mg/L; median 370 mg/L), followed by SO_4 (range 3 - 4460; median 240 mg/L), and HCO_3 (range 0 - 430 mg/L; median 60 mg/L). The highest concentrations of Cl and SO_4 were also measured in the Lluta river basin, with a maximum of 2700 and 4500 mg/L, respectively. The full chemical composition of major and trace elements is shown in Supplementary Materials (Table 1S and Fig. 1S).

The relative abundance of major solute concentrations had an overall pattern Na > Ca > Mg > K and Cl > SO_4 > HCO_3, generally observed in both the Lluta and Codpa-Chaca basins. However, the pattern was slightly different in Camarones valley waters, where K > Mg, and SO4 ~ HCO_3. In the San José basin, the distribution was also different with Ca > Na and SO_4 > HCO_3 > Cl whereas in waters from Altiplanicas basin HCO_3 > SO_4 > Cl, the latter consistent with the predominance of fresher water sources (Appelo and Postma, 2004). The concentrations of Si showed significantly less variability than the major constituents. Overall, the dominant hydrochemical facies were

Na-Cl, Ca-SO_4-Cl, and Ca-HCO_3 water types (Fig. 2S in Supplementary Materials).

4.2.3. Minor and trace constituents

Other elements such as Fe and Al had generally low concentrations (Table 1S in Supplementary Materials) despite localized extremely high values (125 and 260 mg/L, respectively) measured in thermal and surface waters from Azufre river in the Lluta basin near Tacora volcano (Fig. 1B). All concentrations of As, B, and Li were detectable and often high (maximum of 21, 88 and 16 mg/L, respectively), especially in the Camarones and Lluta basins. Concentrations of F were generally low, but the highest measured value was found in geothermal spring waters from Tacora (10 mg/L) and Amuyo (2 mg/L). Generally low concentrations of NO_3, PO_4, and Br were measured with the exception of relatively high NO_3 detected in the Codpa-Chaca (max 74 mg/L) and Lluta basins (max 42 mg/L).

4.2.4. Arsenic speciation

The speciation analysis on recovered fractions by SPE method show that 24% of the studied samples (from a subset of 72 samples >10 μg/L) were dominated by As(III) which contradicted the overall oxidative nature of the waters (Table 3S in Supplementary Materials). The elevated salinity of the samples hindered the application of the SPE method since many of the cartridges were saturated by other elements. The SPE results in many cases showed inconsistent recovery rates, ranging from 0% to 150% with respect to total As measurements (Watts et al., 2010). Conversely, the speciation with HPLC-MS resulted in As(V) the dominant species in 97% of the samples, suggesting the SPE did not represent the speciation of these samples adequately.

4.2.5. O and H stable isotopes ($\delta^{18}O$ and $\delta^{2}H$)

The stable isotopes composition was in the range of -85.5 to -127.2‰ $\delta^{2}H$ and -16.7 to -6.3‰ $\delta^{18}O$ VSMOW. Overall, the lowest values or both isotopes correspond to high altitude samples generally above 4000 m.a.s.l., whereas higher or less negative values did not depend necessarily on the altitude and were in turn related with the source type. Moreover, the highest isotopic signatures were associated with thermal and thermally influenced waters, notably in Camarones basin's Amuyo springs. The full list of stable isotopes analysis results is presented in Table 4S (Supplementary Materials).

4.3. Drinking water quality assessment

A drinking water quality assessment was undertaken on the full set of parameters listed both in the WHO guidelines (WHO,2017) and local potable water regulation (NCh409). This assessment was made considering firstly only samples locally used for drinking ($n = 32$) and also on all samples collected ($n = 90$; Table 5S in Supplementary Materials). It is worth noting that not all the drinking water samples considered have undergone treatment, and in many cases, CS water is directly piped and used without any treatment.

4.3.1. Arsenic and boron occurrence

Approximately 44% of drinking sources contained elevated As, with exceedances of up to 22 times the local regulation and the WHO provisional guideline of 10 μg/L (Figs. 3A and 4A). When all sources are combined, 72% of samples contain elevated As concentrations. On the other side, elevated boron (B > 2.5 g/L) affected 34% of drinking sources and 64% of all samples, respectively.

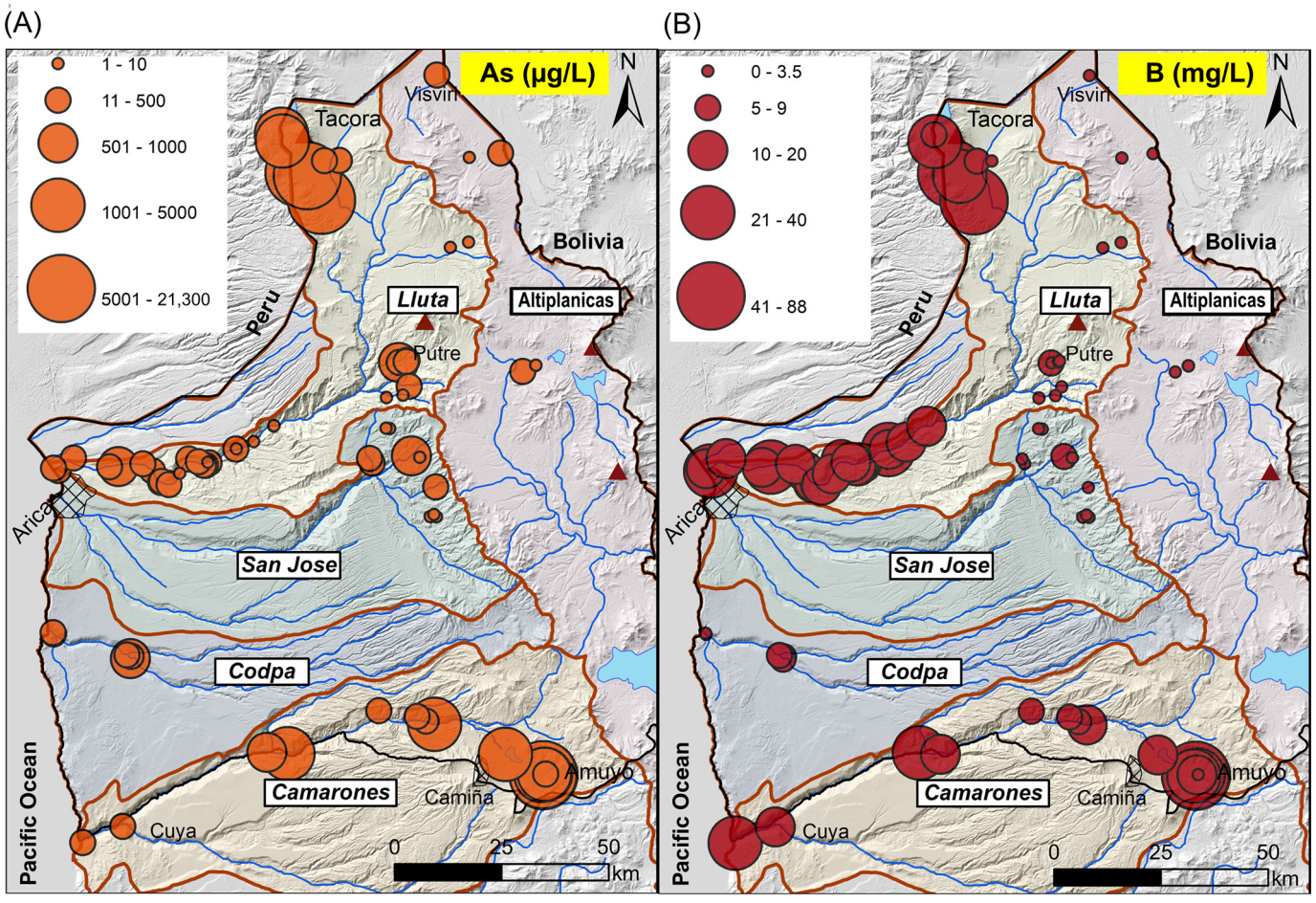

Fig. 3. Map of Arica and Parinacota region illustrating the distribution of concentrations of (A) arsenic (μg/L) and (B) boron (mg/L).

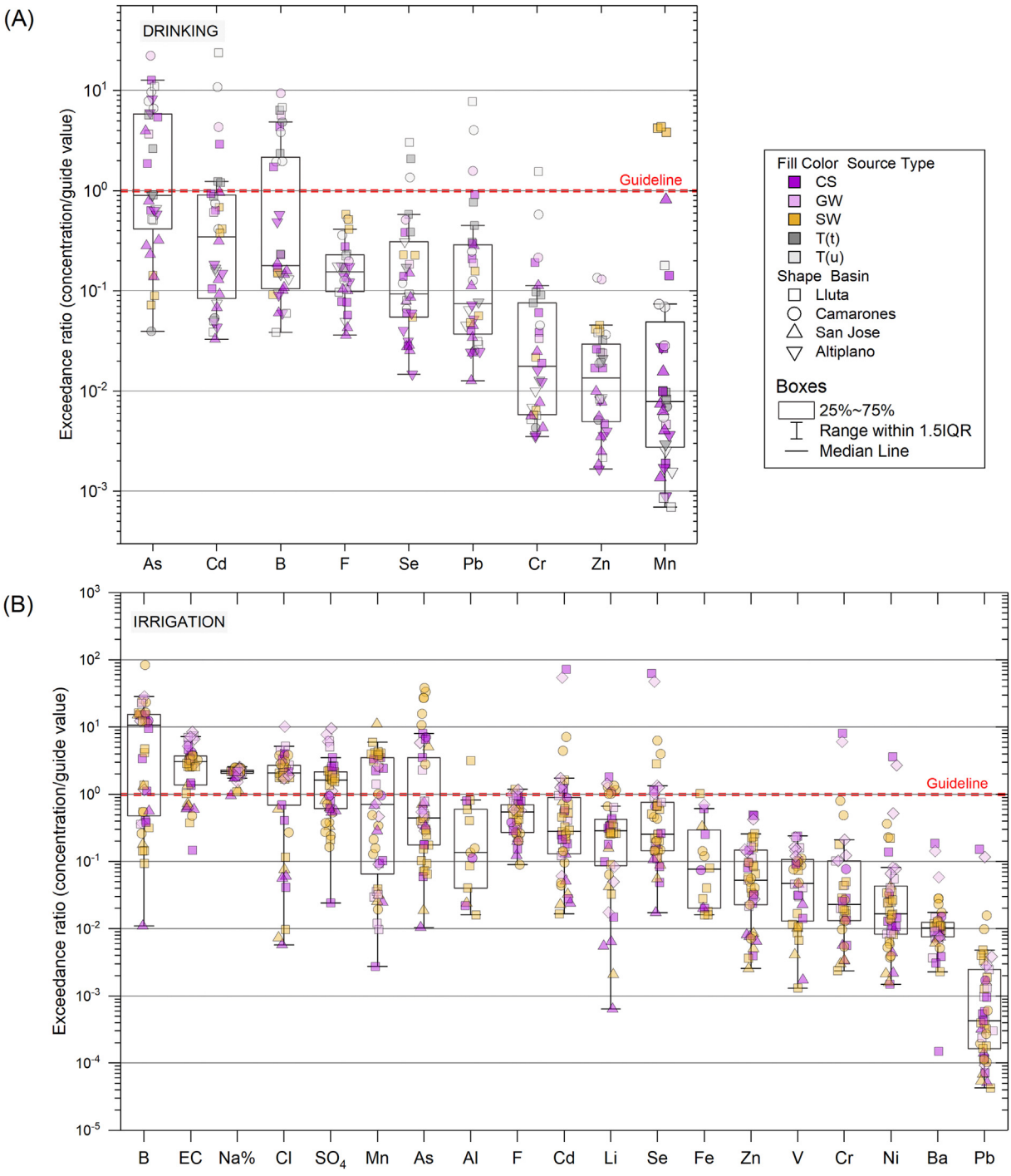

Fig. 4. Exceedance plots and boxes on selected parameters for (A) Samples used for drinking ($n = 32$) – WHO (2017) guideline, (B) Irrigation ($n = 45$) – NCh1333 regulation (Chile). The red dashed line indicates the concentration equals the guideline value (exceedance ratio = 1). On top of this line are plotted all the samples with concentrations above the guideline value. The parameters are ordered according to the median value which is represented by a horizontal line within the boxes, while the whiskers of the boxes represent 1.5 times the interquartile range (IQR). Symbols represent river basins and colours water sources (CS: cold spring, GW: wells, SW: surface waters, T(u) untreated tap). Na% was calculated as 100*Na/[Na + K + Ca + Mg] in meq/L. Thermal springs are not included in this figure since they are not directly used for drinking nor irrigation. (For interpretation of the references to colour in this figure legend, the reader is referred to the web version of this article.)

Of the treated tap waters studied ($n = 5$), most of the parameters were found in compliance with the local and international regulations except for B (Fig. 4A), especially in waters collected in Arica city and Cuyo town (Fig. 1B), both treated by reverse osmosis. However, elevated As was detected in treated tap waters, with values of 26 and 57 μg/L of As in Poconchile and Putre tap water.

The distribution of As and B concentrations (Fig. 3) reveals maximum concentrations of As ~21 mg/L from the Amuyo geothermal springs located in the headwater of the Camarones valley (Fig. 3A), followed by surface water near the Tacora volcano with As ~5 mg/L. The highest concentration of As in Tacora corresponded to SW draining the hydrothermal alteration and abandoned sulphur deposits from previous mining activity (Azufrera, Fig. 2B). Generally lower concentrations of As were measured in samples from cold springs from the San Jose and Lluta valleys.

Elevated concentrations were generally high for most of the samples <2500 m.a.s.l from Lluta and Camarones river (Fig. 3B) with the highest

values measured in geothermal waters from Lluta and Camarones basins. The figure shows that, in general, As and B are similarly distributed, however in the case of B there is less variability in the concentrations in the lower section of Lluta river.

4.3.2. Other parameters of concern

Based on WHO guidelines, in addition to As and B, other relevant parameters (Table 5S in Supplementary Materials) found in potentially harmful concentrations and affecting a substantial number of samples in drinking sources and all samples, were Cd (10% and 42%, respectively), Pb (9% and 28%), Se (3% and 6%), Mn (9% and 33%), and Cr (3% and 10%) (Fig. 4A).

4.4. Irrigation water quality

Several water quality issues in waters used for irrigation (n = 45) were identified (Table 5S in Supplementary Materials), notably elevated B, Cd, As and Se, affecting 89%, 22%, 31%, and 16% of the waters used for irrigation (Fig. 4B). Additionally, elevated salinity (EC > 0.75 mS/cm) affected 80% of irrigation waters, with Na (89%), Cl (73%), and SO_4 (58%) commonly above the local irrigation guidelines (NCh1333). In irrigation waters, B, As, Cd, Se and Mn are found above three times their respective guideline values (Fig. 4B), affecting a similar proportion SW, CS, and GW from the Lluta, Camarones, and Codpa basins. In the Lluta and Camarones valleys, the potential for agricultural activity development is particularly limited by these water quality issues and, in the longer term, soil degradation by accumulation of these elements, notably Na, could affect its future productivity. Salinity risk for irrigation water (Fig. 3S in Supplementary Materials) based on the degradation risk and the overall salinity level (Williams, 1999) shows most irrigation waters fall in the category S2-C4 indicating that soil degradation by cationic exchange and loss of permeability is expected (Williams, 1999).

4.5. Comparison to secondary data compilation

The secondary dataset was reduced to 1503 points meeting the criteria previously discussed in Section 3.3. The main results of this review are shown in Fig. 4S and Table 6S (in Supplementary Materials). Moreover, the results of this data compilation indicate the overall maximum values of many solutes such as Cl, Na, and SO_4 occur in Surire salt flat samples associated with TS discharge from the Altiplanicas basin (Fig. 1B), while elevated concentrations of these solutes were also relevant in the Lluta and Camarones TS waters (Table 7S in Supplementary Materials). Concordia basin (not sampled in our study), had the highest median values for most constituents, this being attributed to localized groundwaters near the coast. The distribution of hydrochemical facies from the samples collected in this study was similar to that evident from secondary data sources (Fig. 5S in Supplementary Materials). However, a greater variability was observed in the secondary data, especially in waters from Lluta and Altiplanicas basins, which is attributed to water sources being from geochemically contrasting fresh CS and saline TS. Consistent with our findings, water types varied with location, with Na-Cl(SO_4) waters dominant in the Camarones, Lluta, and Concordia basins, while Ca-SO_4 type was dominant in the Codpa-Chaca basin and Ca(Na)-HCO_3(SO_4) in the Altiplanicas and San Jose basins.

High-As waters were mostly found in the Camarones, Lluta, and Altiplanicas basins, consistent with the occurrence of geothermal waters in the headwaters of the rivers (Fig. 6S in Supplementary Materials). It is worth noting that in the Camarones river the concentration of As remains elevated in all sections of the main river, in contrast with the Lluta river where a decrease in As is observed downstream. San Jose, Codpa-Chaca and Concordia basins waters were less affected by elevated As, and Altiplanicas showed the greatest variability and maximum values in the Surire salt flat. A substantial proportion of water samples reported in secondary sources were in exceedance of national and international drinking water guidelines, especially for As and B, also consistent with our findings (Fig. 7S in Supplementary Materials). Elevated As concentrations in A&P were widespread affecting 77% of the compiled data ($n = 1288$) with concentrations up to 4200 times greater than the WHO guideline of 10 μg/L. Boron concentrations were above 2.4 mg/L in 44% of the datapoints which included B ($n = 1337$).

5. Discussion and interpretation of geochemical processes

5.1. Correlation of elements and implications for mineral dissolution/precipitation

Molar concentrations of selected parameters were plotted against Cl due to the conservative nature of Cl and the high solubility of Cl-mineral phases (Fig. 8S in Supplementary Materials) (Appelo and Postma, 2004). Solutes plotting on or parallel to the equimolar line (notably Na, K, B) suggest a common origin. Additionally, strong and significant correlations ($r \geq 0.6$, $p \leq 0.05$) between Cl and Na, K, As, B, Ca, Li, Sr, and EC (Table 8S in Supplementary Materials) support that these solutes originate from a common source, such as volcanic rocks weathering and geothermal inputs. Evaporative concentration, evaporites dissolution and/or mixing with brines of volcanic origin may increase the salinity of waters (Risacher et al., 2003) shifting the trend lines towards higher concentrations of Cl.

Other elements such as SO_4 were strongly and significantly correlated with Mg, Mn, Zn, Pb, F, Si, and EC, suggesting that SO_4 is derived from a different source, such as the mineralised areas near volcanic edifices (e.g. sulphate-acid hydrothermal alteration around Tacora volcano in the Lluta basin). In the case of HCO_3 and NO_3 there is no clear linear association with Cl (Fig. 8S in Supplementary Materials), and a nearly vertical trend on SW from the Camarones and Lluta basins is observed to the right of the equimolar line, with Cl remaining almost constant whereas SO_4, HCO_3 and NO_3 vary more substantially. These distributions suggest the precipitation of mineral phases such as gypsum, carbonates, and nitrates, which results in the depletion of these solutes without affecting Cl concentration. Strong and significant correlations between Si and Mg, Mn, Zn, SO_4, and -pH are especially evident in the acidic geothermal waters in the Lluta headwaters. At this location, Si concentrations in the TS samples were greater than in TS samples from Amuyo, indicating that silicate dissolution might have greater importance in the Lluta than the Camarones thermal waters.

The precipitation and dissolution of selected mineral phases were inferred using saturation indices (S.I.; Fig. 9S in Supplementary Materials) shows the proportionally higher dissolution of evaporitic minerals such as gypsum and halite when compared to calcite and fluorite, which reach saturation in some cases, especially in GW. Calcite saturation seems to occur predominantly in the Camarones and Codpa-Chaca basins.

5.2. Principal component analysis

Principal Component Analysis (PCA) on our primary data suggested four components accounted for ~90% of the variance (based on eigenvalues from correlation matrix) (Table 9S-A; Fig. 10S-A in Supplementary Materials). Two groupings of samples are generally associated with altitude. Waters from fresh sources at higher altitude generally trend towards the left side of the diagram and are closely associated with HCO_3, pH, and Si. This group largely corresponds to CS and SW, especially from the Altiplanicas, San Jose and Lluta basins. Furthermore, the association between Na-Cl-As-B is plotted on the upper-right quadrant with the Ca-Mg-SO4 association evident in the bottom-right. This behaviour was confirmed by a hierarchical cluster analysis (HCA) represented in a dendrogram (Fig. 10S-B in Supplementary Materials). In this diagram, three clusters of parameters are observed, viz. pH-HCO_3-Si, Na-Cl-B-K-As-EC, and Ca-SO_4-Mg. These associations suggest that

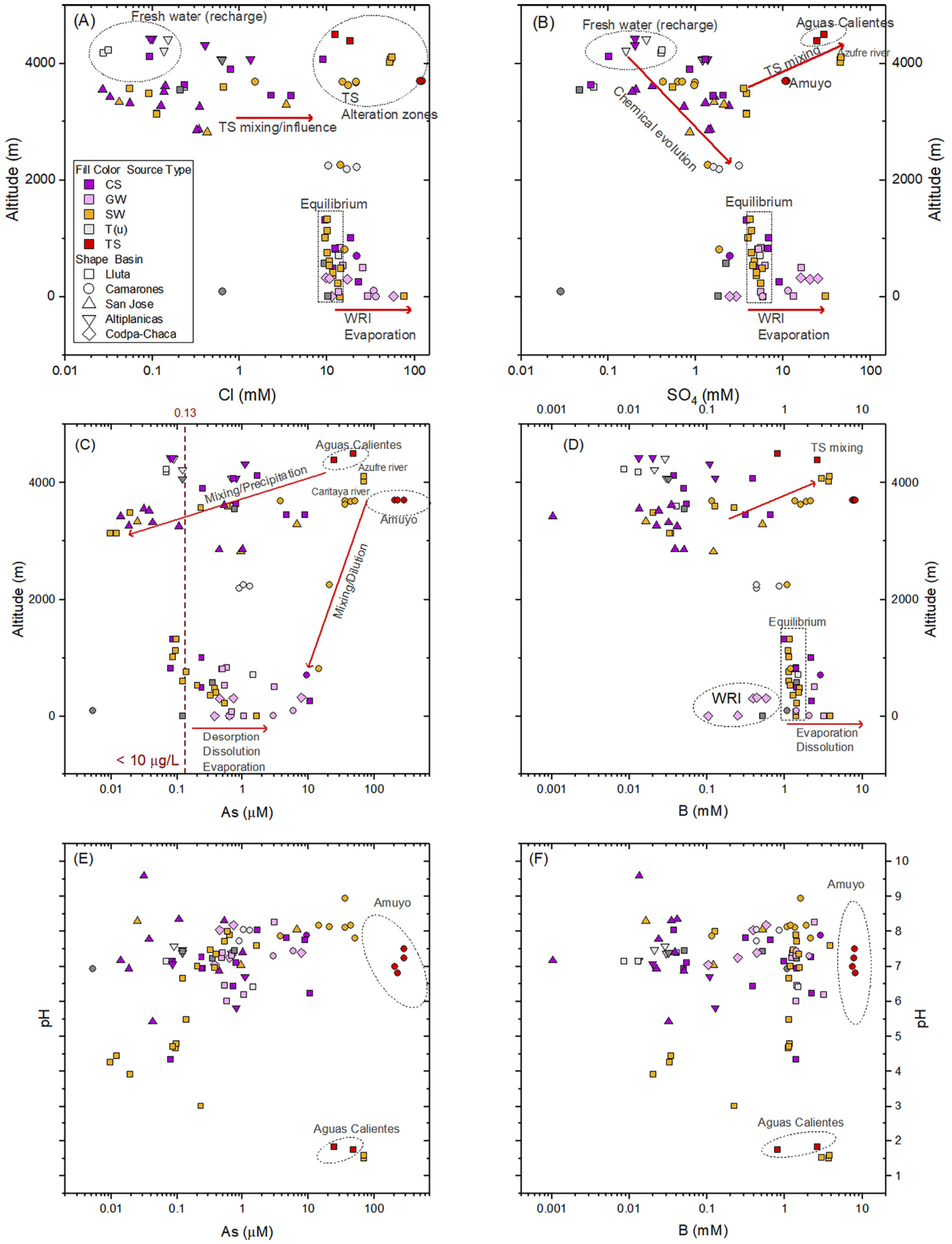
(A)
Fresh water (recharge)
TS
Alteration zones
TS mixing/influence
Fill Color Source Type
CS
GW
SW
T(u)
TS
Shape Basin
Lluta
Camarones
San Jose
Altiplanicas
Codpa-Chaca
Equilibrium
WRI
Evaporation
Altitude (m)
Cl (mM)
(B)
Fresh water (recharge)
Aguas Calientes
Azufre river
TS mixing
Amuyo
Chemical evolution
Equilibrium
WRI
Evaporation
SO4 (mM)
(C)
0.13
Aguas Calientes
Azufre river
Mixing/Precipitation
Caritaya river
Amuyo
Mixing/Dilution
Desorption
Dissolution
Evaporation
< 10 µg/L
As (µM)
(D)
TS mixing
Equilibrium
WRI
Evaporation
Dissolution
B (mM)
(E)
Amuyo
Aguas Calientes
pH
As (µM)
(F)
Amuyo
Aguas Calientes
pH
B (mM)

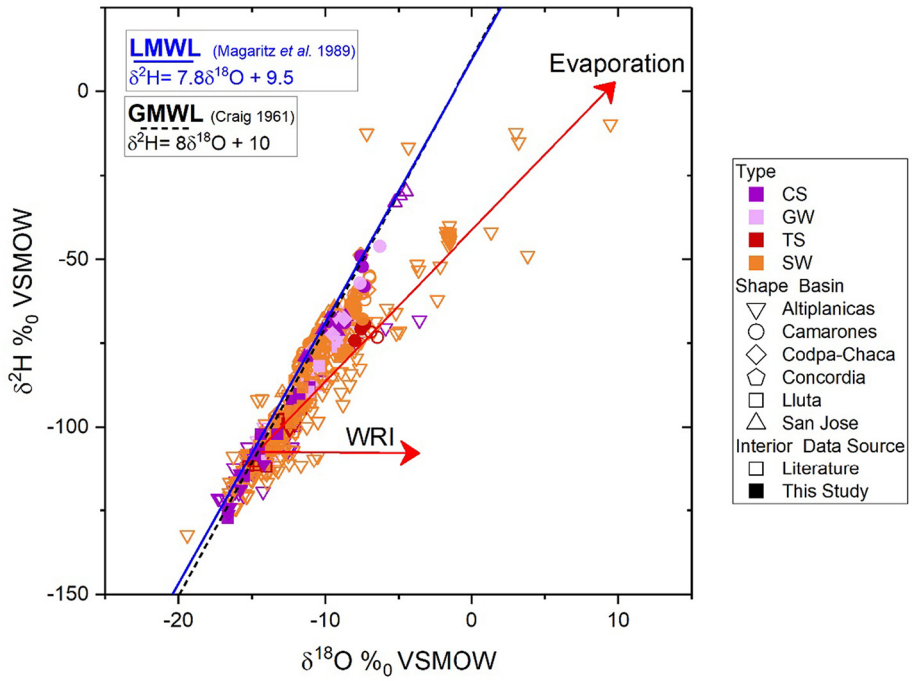

Fig. 6. Diagram of δ^2H vs $\delta^{18}O$ (‰ VSMOW) of the existing hydrochemical data (Table 4-6S) contrasted with the existing data (Arrau, 1997; Herrera et al., 2006; Tassi et al., 2010; DGA-Mayco, 2013; CNR-GeoHidrologia Consultores, 2014; DGA-AMEC, 2014; DGA-Matraz Consultores, 2015; DGA-Con Potencial Consultores, 2016; DGA-ICASS, 2016, 2017). The main processes (evaporation and water-rock interaction) causing deviation from the Local Meteoric Water Line (LMWL) (Magaritz et al., 1989) and Global Meteoric Water Line (GMWL) (Craig, 1961) are indicated.

the most important geochemical processes are silicate weathering, halite dissolution, brine mixing, and/or gypsum dissolution, respectively.

5.3. Fate of arsenic and boron: altitude variation

To study the trends in chemical evolution in water composition along dominant flowpaths, a series of plots of selected elements concentration versus altitude were plotted for all the basins (Fig. 5). Overall, the concentrations of Cl (Fig. 5A), SO_4 (Fig. 5B), As (Fig. 5C), and B (Fig. 5D), form clusters depending on the altitude of the samples. Two domains are identified:

A. Above 2000 m.a.s.l.: This group shows the greatest variability of concentrations, roughly between a fresher source (mainly CS and SW) and more saline end-member (TS and hydrothermal alteration water) (Fig. 5). This is particularly noted in waters from the Lluta and Camarones basins where two contrasting thermal end-members are evident (Tacora/Aguas Calientes and Amuyo Springs).
B. Below 2000 m.a.s.l.: This group is characterized by samples that have reached or are close to equilibrium (as suggested by roughly constant concentrations of major anions) representing more chemically evolved waters with nearly constant concentrations of Cl (Fig. 5A), SO_4 (Fig. 5B), and B (Fig. 5D and F). Deviations from this trend may be due to evaporation and dissolution of minerals from sediments and are notably observed in B concentrations in GW from Codpa-Chaca. The case of As is slightly different, especially for SW from the Lluta river where concentrations of As visibly increase in lower areas (Fig. 5D), likely derived from desorption, dissolution, and/or evaporation processes, as suggested by an increase in pH (Fig. 5E).

In Camarones river waters, the concentrations of As show a slight decrease towards lower sections of the river, especially in GW.

5.4. Origin of waters

In addition to chemical composition, stable isotope data δ^2H and $\delta^{18}O$ (Fig. 6) from this study and secondary sources reveals a contrasting origin of waters from the basins within A&P. Most samples have an isotopic signature in the range of -50 to -125‰ δ^2H and -16 to -5‰ $\delta^{18}O$ VSMOW (Fig. 6). This signature is consistent with high altitude rain and snow, plotting in a slightly shifted trend in comparison to the global and local meteoric line (Magaritz et al., 1989). Samples from Altiplanicas show signs of isotopic enrichment by evaporation and are consistent with a closed basin signature (Craig, 1961). Geothermal waters, notably from Amuyo Springs in Camarones Valley, were among the most enriched and plotted within the path of evaporated waters. The greatest isotopic enrichment from the studied samples corresponds to SW suggesting they undergo more evaporation than TS, GW, and CS.

5.5. Summary of main geochemical controls and conceptual model

The main identified geochemical controls on the composition of waters in A&P show an important dependence on the presence of geothermal springs and on the location: primarily by altitude and secondarily by basin (Figs. 7 and 8). Overall, two end-members were identified: (i) low salinity (molar ratio Na + K/Cl > 10) and Ca-HCO_3 waters from CS at high altitude (>2000 m.a.s.l) where rainfall and snowfall take place, and (ii) high salinity (molar ratio Na + K/Cl ~ 1) TS and evaporated waters (Fig. 7A). Most SW and GW samples plot along the equimolar line between Na/Cl representing different degrees of halite

Fig. 5. Scatter plots of concentrations of selected parameters (molar) with respect to sampling altitude (m.a.s.l.), including (A) Cl, (B) SO4, (C) As, and (D) B; and with respect to pH (E) As and (F) B. Symbols represent river basins and colours water sources (CS: cold spring, GW: wells, SW: surface waters, T(u) untreated tap, TS: thermal springs).

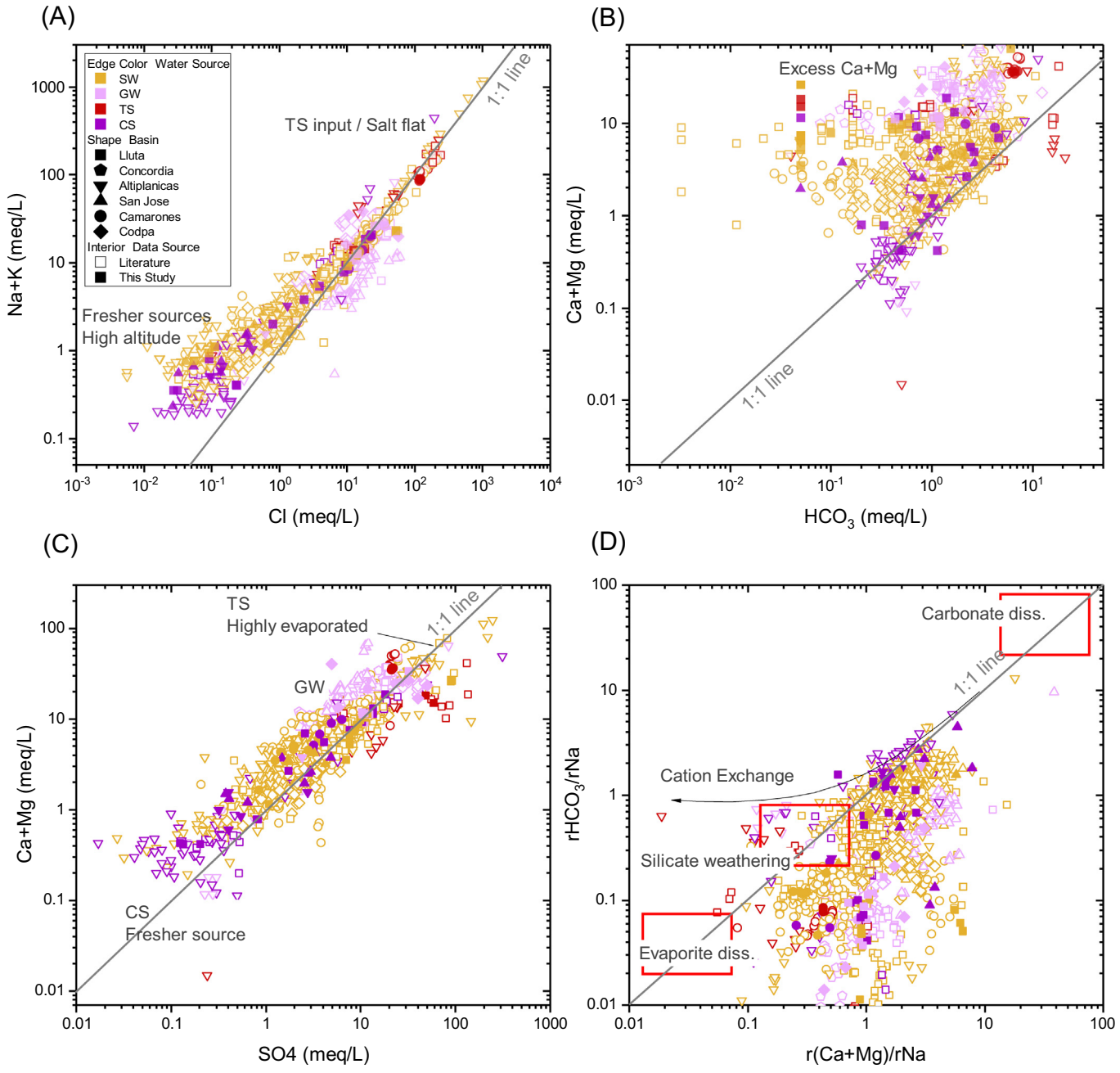

Fig. 7. Diagrams summarising the main geochemical processes controlling major elements composition of studied waters (in meq/L; Gaillardet et al., 1999). 1:1 line represents chemical reactions between (a) Na + K vs Cl – halite dissolution and mixing with geothermal brines (b) Ca + Mg vs HCO_3 – dissolution of carbonates and controls on high altitude waters (c) Ca + Mg vs SO_4 – gypsum dissolution with particular influence in groundwaters (d) summary of main geochemical processes – dissolution of carbonates, silicate weathering, and dissolution of evaporites.

dissolution and brines mixing between these two endmembers. Additionally, gypsum dissolution/precipitation is also an important control on water chemistry and is especially relevant in GW composition (Fig. 7C). Dissolution and precipitation of carbonates appear less relevant, except for samples from CS notably in high altitude areas (Fig. 7B). The excess of Ca and Mg observed in this plot is likely derived from gypsum dissolution and other water-rock interaction processes (e.g. silicate weathering) (Fig. 7D).

The different chemical composition of the studied waters was determined by altitude and source type and suggests different degrees of mixing between freshwater sources from high altitude areas with geothermal waters and/or interactions with hydrothermal alteration rocks. The sources of As, B, and other solutes is the leaching of andesitic to dacitic rocks (water rock interactions), deep brine circulation, and input of volcanic fluids (degasification) (Risacher et al., 2011; García et al., 2017; Tapia et al., 2019). Moreover, the type of geothermal input and degree of evaporation are key to determine the concentration and fate of As and other metal/oids along the course of the main river systems studied (Fig. 8).

The maximum As and B concentrations in the A&P region have been measured in Andean closed (endorheic) basins and salt flats (Fig. 8, area 1; Lagos Durán, 2016; Tapia et al., 2021). In exorheic systems such as the Lluta and Camarones basin, evaporation has a lesser impact than in closed basins. The most relevant contrast between these rivers is the type of geothermal input in the headwaters, which is suggested to determine the fate of As concentration downstream. Lluta TS waters, notably *Aguas Calientes* spring near Tacora volcano, were of an acid-SO_4 nature (rich in Fe, Al, and Si) and were associated with direct volcanic

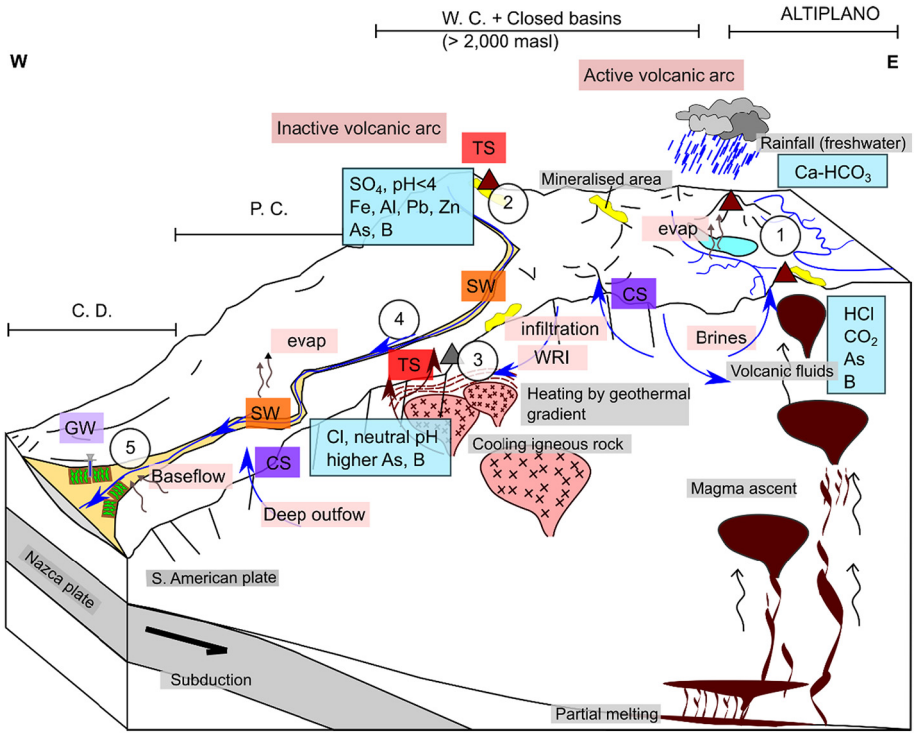

Fig. 8. Conceptual model of main geochemical processes controlling chemical composition and As occurrence of waters in the A&P region. The sketch (not to scale) is shown as an EW section and includes both deep and surface processes (including morphological units: C.D.: Central Depression, P.C.: Pre-Cordillera, W·C: Western Cordillera, and Altiplano). At depth, the main processes are the subduction of the Nazca plate under the South American plate. A result of this process is the partial melting of the mantle and formation and ascent of magma forming an active volcanic front. The main surface processes and sections are indicated in numbers: (1) thermal/volcanic input, intense evaporation and formation of salt flats in closed basins (e.g. Surire); (2) interaction of freshwater with mineralised areas and/or mixing with acid-SO_4 waters near active volcanoes (e.g. Tacora area); (3) neutral Na-Cl geothermal waters input from deep circulation and brines mixing (water rock interaction and leaching of host rocks); (4) surface runoff and mixing with deep outflow cold springs (while increasing pH); (5) lower section of valleys with contribution of baseflow and accumulation of As in sediments.

input and shallow water circulation (Fig. 8, area 2; Capaccioni et al., 2011). Conversely, Camarones TS, notably the *Amuyo* geothermal springs were of a Na-Cl near-neutral nature (low Fe, Al), and were associated with the deeper circulation of waters and leaching of the host rocks (Fig. 8, area 3; Risacher et al., 2011; López et al., 2012; Tapia et al., 2021). The concentration of As in Lluta rapidly decreases during the mixing with cold springs, tributaries, interaction with sediments, and the increase of pH in the Lluta river (Fig. 8, area 4; Leiva et al., 2014; Guerra et al., 2016). In the Camarones river, the concentration of As remains relatively constant downstream (Cornejo et al., 2004), probably due to the lower abundance of elements that may capture As onto precipitates (Fig. 5C).

The pattern described above is observed in most of the SW in the Lluta and Camarones basins. However, SW and GW show different behaviour in the lower areas (Fig. 8, area 5). In the Lluta river the salinity and concentration of As increases in lower areas indicating the likely release from As-rich sediments of the river bed which have been previously identified in the area (Fig. 2B) (Lacassie et al., 2014) and/or by groundwater baseflow to the river, thus hindering water uses. This generally occurs at higher pH typical of waters exhibiting alkali desorption in oxidising environments (Smedley and Kinniburgh, 2002). On the other hand, in Camarones, GW collected near the coast show lower concentrations of As in comparison to river water, suggesting that part of the As is adsorbed onto sediments within the aquifers, which is also consistent with the high As concentration in sediments found in this valley (Baeza et al., 2015).

6. Conclusions

Through the sampling of waters and the compilation of existing secondary hydrochemical data from all six basins within the Arica and Parinacota region, we have identified water quality issues and proposed the main geochemical controls on the composition of waters from different source-types, altitudes, and river basins. Potentially harmful concentrations of As, Cd, Pb, F, and B were detected. Notably, elevated (> 10 μg/L) As was found in 72% of all samples collected ($n = 90$) in rural areas within the A&P region and in 44% of samples indicated as drinking sources ($n = 32$). Additionally, surface waters from Lluta and the Camarones river show unfavourable compositions for their use in irrigation, due to risks of soil and plant damage by elevated Na and high concentrations of B.

Overall, the composition of the samples was strongly controlled by mixing with geothermal waters, evaporative concentration, and the dissolution of minerals, notably halite, gypsum, and calcite. The trends observed in water composition suggest a close relation between the nature of geothermal springs (Na-Cl and SO_4 waters) in the headwaters of the river basins and the magnitude and fate of As occurrence. This was particularly clear in Lluta and Camarones waters, which showed important differences with SO_4 contributing the most in explaining the variance in compositions in Lluta basin; while Na, Cl and B were more important in the Camarones valley. Additionally, a clear separation between high altitude and low altitude domains was found. In high altitude areas, the presence of metals was controlled by the direct input from geothermal water and interaction with hydrothermal alteration and volcanic deposits, adding As, B, and Li to the waters. Conversely, in topographically lower areas, the main controls were the dissolution of gypsum, evaporation, and the interaction with sediments in the riverbed and aquifers, often increasing As concentrations near the coast in Lluta basin groundwaters, while B remained roughly constant. This work shows that despite the common volcanic/geothermal origin of As, variations in the type of water determine the magnitude and fate of As occurrence. This work also contributes to the further understanding of the geochemical controls on water composition within the A&P region. Some of the processes and interpretations could be

applicable in arid zones impacted by elevated As and B elsewhere in Chile and/or internationally.

CRediT authorship contribution statement

G.P. Pincetti-Zuniga: Conceptualization, Funding acquisition, Methodology, Software, Formal analysis, Investigation, Visualization, Writing – original draft. **L.A. Richards:** Conceptualization, Funding acquisition, Investigation, Supervision, Writing – review & editing. **L. Daniele:** Funding acquisition, Resources, Writing – review & editing. **A.J. Boyce:** Formal analysis, Resources, Writing – review & editing. **D.A. Polya:** Conceptualization, Supervision, Funding acquisition, Writing – review & editing.

Declaration of competing interest

The authors declare that they have no known competing financial interests or personal relationships that could have appeared to influence the work reported in this paper.

Acknowledgements

GP acknowledges funding from National Agency for Research and Development (ANID)/Scholarship Program/DOCTORADO BECAS CHILE 2016/Folio 72170419, with additional support from the University of Manchester FSE Social Responsibility Fund 2017/18 awarded to GP, LR and DP. LR was supported by the Leverhulme Trust (ECF2015-657) and a University of Manchester Dame Kathleen Ollerenshaw Fellowship. LD acknowledges funding by FONDAP no. 15200001 (Centro de Excelencia en Geotermia de los Andes, CEGA), ICM no. NC130065 (Núcleo Milenio Trazadores de Metales, NMTM). We thank Paul Lythgoe and Alastair Bewsher for analytical support. The Natural Environment Research Council (NERC) and Isotope Geosciences Facilities Steering Committee (NIGFSC) are acknowledged for their support on the isotopic analysis (grant IP-1925-0619 to GP, LR, DP and AB). We thank the staff at the Scottish Universities Environment Research Centre (SUERC) for their support on analytical procedures on stable isotopes analysis. We are very grateful to the substantial field and logistical support especially from Eduardo Garrido, Richard Fernandez, Sergio Miranda, Junta de Vigilancia del Río Lluta and local authorities and landowners. Thanks to the anonymous reviewers for their contributions to improving this manuscript.

Appendix A. Supplementary data

Supplementary data to this article can be found online at https://doi.org/10.1016/j.scitotenv.2021.150206.

References

Allende, K.L., McCarthy, D.T., Fletcher, T.D., 2014. The influence of media type on removal of arsenic, iron and boron from acidic wastewater in horizontal flow wetland microcosms planted with Phragmites australis. Chem. Eng. J. 246, 217–228. https://doi.org/10.1016/j.cej.2014.02.035.

Appelo, C.A.J., Postma, D., 2004. Geochemistry, Groundwater and Pollution. Second Edi. Taylor & Francis https://doi.org/10.1201/9781439833544.

Arrau, L., 1997. Modelo de simulacion hidrológico operacional Cuenca del río San José. Informe técnico. [WWW Document] . https://snia.mop.gob.cl/sad/REH599_v1.pdf.

Arriaza, B., Amarasiriwardena, D., Cornejo, L., Standen, V., Byrne, S., Bartkus, L., Bandak, B., 2010. Exploring chronic arsenic poisoning in pre-columbian chilean mummies. J. Archaeol. Sci. 37, 1274–1278. https://doi.org/10.1016/j.jas.2009.12.030.

Arriaza, B., Amarasiriwardena, D., Standen, V., Yáñez, J., Van Hoesen, J., Figueroa, L., 2018. Living in poisoning environments: invisible risks and human adaptation. Evol. Anthropol. Issues, News, Rev. 27, 188–196. https://doi.org/10.1002/evan.21720.

Baeza, L., Lacassie, J.P., Astudillo, F., Barrera, J., Carrasco, F., Castillo, P., Figueroa, M., Miralles, C., Muñoz, N., Ramirez, C., Salinas, P., 2015. Anomalías geoquímicas de sedimentos de drenaje de la Hoja Arica, Región de Arica y Parinacota. XV Congreso Geológico Chileno, pp. 1–4. https://biblioteca.sernageomin.cl/opac/datafiles/14905_v3_pp_268_271.pdf.

Bhattacharya, P., Jacks, G., Frisbie, S.H., Smith, E., Naidu, R., Sarkar, B., 2002. Arsenic in the environment: a global perspective. In: Sarkar, B. (Ed.), Heavy Metals In The Environment. Marcel Dekker, Inc, Toronto, Ontario, Canada, pp. 147–216.

Borgono, J.M., Vicent, P., Venturino, H., Infante, A., 1977. Arsenic in the drinking water of the city of Antofagasta: epidemiological and clinical study before and after the installation of a treatment plant. Environ. Health Perspect. 19, 103–105. https://doi.org/10.1289/ehp.19-1637404.

Bundschuh, J., Litter, M.I., Parvez, F., Román-Ross, G., Nicolli, H.B., Jean, J.S., Liu, C.W., López, D., Armienta, M.A., Guilherme, L.R.G., Cuevas, A.G., Cornejo, L., Cumbal, L., Toujaguez, R., 2012. One century of arsenic exposure in Latin America: a review of history and occurrence from 14 countries. Sci. Total Environ. 429, 2–35. https://doi.org/10.1016/j.scitotenv.2011.06.024.

Byrne, S., Amarasiriwardena, D., Bandak, B., Bartkus, L., Kane, J., Jones, J., Yañez, J., Arriaza, B., Cornejo, L., 2009. Were Chinchorros Exposed to Arsenic? Arsenic Determination in Chinchorro Mummies' Hair by Laser Ablation Inductively Coupled Plasma-mass Spectrometry (LA-ICP-MS). https://doi.org/10.1016/j.microc.2009.08.006.

Caceres, D.D., Pino, P., Montesinos, N., Atalah, E., Amigo, H., Loomis, D., 2005. Exposure to inorganic arsenic in drinking water and total urinary arsenic concentration in a chilean population. Environ. Res. 98, 151–159. https://doi.org/10.1016/j.envres.2005.02.007.

Capaccioni, B., Aguilera, F., Tassi, F., Darrah, T., Poreda, R.J., Vaselli, O., 2011. Geochemical and isotopic evidences of magmatic inputs in the hydrothermal reservoir feeding the fumarolic discharges of tacora volcano (northern Chile). J. Volcanol. Geotherm. Res. 208, 77–85. https://doi.org/10.1016/j.jvolgeores.2011.09.015.

Clarke, J.D.A., 2006. Antiquity of aridity in the chilean Atacama Desert. Geomorphology 73, 101–114. https://doi.org/10.1016/j.entcs.2005.12.035.

CNR-GeoHidrologia Consultores, 2014. Diagnóstico de la Subcuenca Aportante al Embalse Caritaya Región de Arica y Parinacota [WWW document]. URL http://bibliotecadigital.ciren.cl/handle/123456789/26339.

Copaja, S.V., Muñoz, F.J., Copaja, S.V., Muñoz, F.J., 2018. Heavy metals concentration in sediment of lluta river basin. J. Chil. Chem. Soc. 63, 3878–3883. https://doi.org/10.4067/s0717-97072018000103878.

Cornejo, L., Mansilla, H.D., Arenas, M.J., Flores, V., Figueroa, L., 2004. Removal of arsenic from waters of the Camarones River, Arica, Chile, using the modified SORAS technology. In: Litter, M.I., Mansilla, H.D. (Eds.), Advances in Low-Cost Technologies for Disinfection, Decontamination and Arsenic Removal in Waters from Rural Communities of Latin America (HP and SORAS Methods) - ASO Project AE. 141, pp. 85–97.

Cornejo, L., Lienqueo, H., Arenas, M., Acarapi, J., Contreras, D., Yáñez, J., Mansilla, H.D., 2008. In field arsenic removal from natural water by zero-valent iron assisted by solar radiation. Environ. Pollut. 156, 827–831. https://doi.org/10.1016/j.envpol.2008.05.022.

Cornejo, L., Lienqueo, H., Vilca, P., 2019. Hydro-chemical characteristics, water quality assessment and water relationship (HCA) of the Amuyo Lagoons, Andean Altiplano, Chile. Desalin. Water Treat. 153, 36–45. https://doi.org/10.5004/dwt.2019.24014.

Cornejo-Ponce, L., Acarapi-Cartes, J., 2011. Fractionation and bioavailability of arsenic in agricultural soils: solvent extraction tests and their relevance in risk assessment. J. Environ. Sci. Health A Tox. Hazard. Subst. Environ. Eng. 46, 1247–1258. https://doi.org/10.1080/10934529.2011.598807.

Craig, H., 1961. Isotopic variations in meteoric waters. Science 133, 1702–1703. https://doi.org/10.1126/science.133.3465.1702.

DGA, 2020. Servicios hidrometeorologicos DGA [WWW document]. https://dga.mop.gob.cl/servicioshidrometeorologicos/Paginas/default.aspx.

DGA-AMEC, 2014. Estudio Caracterización Hidrogeológica de la cuenca del río Colpitas, XV Región [WWW document]. URL https://snia.mop.gob.cl/sad/SUB-5623.pdf.

DGA-Arrau Ingeniería, 2013. Estudio básico diagnóstico de obras hidráulicas y fluviales quebrada de Camarones, Región de Arica y Parinacota [WWW document]. URL https://snia.mop.gob.cl/sad/REH5718v1.pdf.

DGA-Con Potencial Consultores, 2016. Estudio diagnóstico de disponibilidad hídrica Cuenca del río Camarones [WWW document]. https://snia.mop.gob.cl/sad/REH5718v1.pdf.

DGA-DICTUC, 2008. Propuesta De Calidad Objetivo Y Analisis General De Impacto Economico Y Social-Cuenca Rio Lluta . Bases Conceptuales Y Cuantitativas . [WWW document]. URL https://snia.mop.gob.cl/sad/CQA5005.pdf.

DGA-ICASS, 2016. Análisis integral de soluciones a la escasez hídrica, región de Arica y Parinacota (primera parte) [WWW document]. URL https://www.repositoriodirplan.cl/handle/20.500.12140/25849?show=full.

DGA-ICASS, 2017. Análisis integral de soluciones a la escasez hídrica, región de Arica y Parinacota (segunda parte) [WWW document]. URL https://snia.mop.gob.cl/sad/REH5578v1.pdf.

DGA-Matraz Consultores, 2015. Diagnóstico de disponibilidad hídrica en la Cuenca del Río Lauca, Región de Arica y Parinacota. [WWW document]. URL https://snia.mop.gob.cl/sad/REH5578v1.pdf.

DGA-Mayco, 2013. Balance Hídrico en sectores acuíferos de mediana criticidad (Quebrada Chaca-Vitor) [WWW document]. URL https://www.repositoriodirplan.cl/handle/20.500.12140/25873.

DIVA-GIS, 2020. Download data by country | DIVA-GIS [WWW document]. URL http://www.diva-gis.org/gdata (accessed 9.20.20).

DOH-R&Q ingeniería, 2012. Estudio de Impacto Ambiental: Proyecto "Embalse Chironta" XV Región de Arica y Parinacota, Comuna de Arica [WWW document]. URL https://infofirma.sea.gob.cl/DocumentosSEA/MostrarDocumento?docId=36/da/74e3c6ca1716d9e921c79de217eaef56ed5b.

Farnham, I.M., Singh, A.K., Stetzenbach, K.J., Johannesson, K.H., 2002. Treatment of nondetects in multivariate analysis of groundwater geochemistry data. Chemom. Intell. Lab. Syst., 265–281 https://doi.org/10.1016/S0169-7439(01)00201-5.

Ferraris, F., Vila, T., 1990. Volcanic sulfur deposits in the Andes of northern Chile. Stratabound Ore Deposits in the Andes. Springer, Berlin Heidelberg, Berlin, Heidelberg, pp. 691–701 https://doi.org/10.1007/978-3-642-88282-1_55.

Ferreccio, C., Gonzalez, C., Milosavjlevic, V., Marshall, G., Sancha, A.M., Smith, A.H., 2000. Lung cancer and arsenic concentrations in drinking water in Chile. Epidemiology 11, 673–679. https://doi.org/10.1097/00001648-200011000-00010.

Gaillardet, J., Dupré, B., Louvat, P., Allègre, C.J., 1999. Global silicate weathering and CO2 consumption rates deduced from the chemistry of large rivers. Chem. Geol. 159, 3–30. https://doi.org/10.1016/S0009-2541(99)00031-5.

García, M., Gardeweg, M., Clavero, J., Hérail, G., 2004. Hoja Arica. Escala 1:250.000. Carta Geológica de Chile, Serie Geología Básica. Servicio Nacional de Geología y Minería.

García, M.G., D'Hiriart, J., Giullitti, J., Lin, H., Custo, G., Hidalgo, M.D.V., Litter, M.I., Blesa, M.A., 2004. Solar light induced removal of arsenic from contaminated groundwater: the interplay of solar energy and chemical variables. Sol. Energy 77, 601–613. https://doi.org/10.1016/j.solener.2004.06.022.

García, M., Maksaev, V., Townley, B., Dilles, J., 2017. Metallogeny, structural evolution, post-mineral cover distribution and exploration in concealed areas of the northern chilean Andes. Ore Geol. Rev. 86, 652–672. https://doi.org/10.1016/j.oregeorev.2017.01.025.

Guerra, P., Gonzalez, C., Escauriaza, C., Pizarro, G., Pasten, P., 2016. Incomplete mixing in the fate and transport of arsenic at a river affected by acid drainage. Water Air Soil Pollut. 227. https://doi.org/10.1007/s11270-016-2767-5.

Hem, J.D., 1985. Study and Interpretation the Chemical of Natural of Characteristics Water, U.S. Geological Survey Water-Supply Paper.

Herrera, C., Pueyo, J.J., Sáez, A., Valero-Garcés, B.L., 2006. Relación de aguas superficiales y subterráneas en el área del lago Chungará y lagunas de cotacotani, norte de Chile: un estudio isotópico. Rev. Geol. Chile 33, 299–325. https://doi.org/10.4067/s0716-02082006000200005.

Hopenhayn-Rich, C., Browning, S.R., Hertz-Picciotto, I., Ferreccio, C., Peralta, C., Gibb, H., 2000. Chronic arsenic exposure and risk of infant mortality in two areas of Chile. Environ. Health Perspect. 108, 667–673. https://doi.org/10.2307/3434889.

Houston, J., Hartley, A.J., 2003. The central andean west-slope rainshadow and its potential contribution to the origin of hyper-aridity in the Atacama Desert. Int. J. Climatol. 23, 1453–1464. https://doi.org/10.1002/joc.938.

INE, 2018. Censo 2017 [WWW Document]. Inst. Nac. Estadísticas. http://resultados.censo2017.cl/Region?R=R15.

INH, 2014. Caracterización de la Cuenca del río San José para la implementación de un programa de recarga artificial de acuíferos [WWW document]. URL https://www.repositoriodirplan.cl/handle/20.500.12140/25713.

INN, 2006. Norma Chilena Oficial NCh409/1.Of2005 [WWW document]. Inst. Nac. Norm. https://ciperchile.cl/pdfs/11-2013/norovirus/NCh409.pdf.

Inostroza, M., Tassi, F., Aguilera, F., Sepúlveda, J.P., Capecchiacci, F., Venturi, S., Capasso, G., 2020. Geochemistry of gas and water discharge from the magmatic-hydrothermal system of guallatiri volcano, northern Chile. Bull. Volcanol. 82. https://doi.org/10.1007/s00445-020-01396-2.

JICA, 1995. The study on the development of water resources in Northern Chile: main report [WWW document]. Japan Int. Coop. Agency. http://open_jicareport.jica.go.jp/pdf/11189446_01.pdf.

Khan, K.M., Chakraborty, R., Bundschuh, J., Bhattacharya, P., Parvez, F., 2020. Health effects of arsenic exposure in Latin America: an overview of the past eight years of research. Sci. Total Environ. 710, 136071. https://doi.org/10.1016/j.scitotenv.2019.136071.

Lacassie, J.P., Astudillo, F., Baeza, L., Carrasco, F., Castillo, P., Espinoza, F., Figueroa, M., Miralles, C., 2014. Anomalías Geoquímicas en el norte grande y norte Chico [WWW document]. http://sitiohistorico.sernageomin.cl/pdf/presentaciones-geo/Mapa-geoquimico-del-Norte-de-Chile.pdf.

Lagos Durán, L.V., 2016. Hidrogeoquímica de fuentes termales en ambientes salinos relacionados con salares en los Andes del norte de Chile [WWW document]. MSc Thesis. URL http://repositorio.uchile.cl/handle/2250/140833.

Leiva, E.D., Rámila, C.D.P., Vargas, I.T., Escauriaza, C.R., Bonilla, C.A., Pizarro, G.E., Regan, J.M., Pasten, P.A., 2014. Natural attenuation process via microbial oxidation of arsenic in a high Andean watershed. Sci. Total Environ. 466–467, 490–502. https://doi.org/10.1016/j.scitotenv.2013.07.009.

Litter, M.I., Alarcón-Herrera, M.T., Arenas, M.J., Armienta, M.A., Avilés, M., Cáceres, R.E., Cipriani, H.N., Cornejo, L., Dias, L.E., Cirelli, A.F., Farfán, E.M., Garrido, S., Lorenzo, L., Morgada, M.E., Olmos-Márquez, M.A., Pérez-Carrera, A., 2012. Small-scale and household methods to remove arsenic from water for drinking purposes in Latin America. Sci. Total Environ. 429, 107–122. https://doi.org/10.1016/j.scitotenv.2011.05.004.

López, D.L., Bundschuh, J., Birkle, P., Armienta, M.A., Cumbal, L., Sracek, O., Cornejo, L., Ormachea, M., 2012. Arsenic in volcanic geothermal fluids of Latin America. Sci. Total Environ. 429, 57–75. https://doi.org/10.1016/j.scitotenv.2011.08.043.

Magaritz, M., Aravena, R., Peña, H., Suzuki, O., Grilli, A., 1989. Water chemistry and isotope study of streams and springs in northern Chile. J. Hydrol. 108, 323–341. https://doi.org/10.1016/0022-1694(89)90292-8.

Mahan, D., Waissblut, O., Cáceres, D., 2020. Carcinogenic and non-carcinogenic health risks of arsenic exposure in drinking water in the rural environment. Glob. J. Environ. Sci. Manag. 6, 165–174. https://doi.org/10.22034/gjesm.2020.02.03.

Marengo, J.A., Liebmann, B., Grimm, A.M., Misra, V., Silva Dias, P.L., Cavalcanti, I.F.A., Carvalho, L.M.V., Berbery, E.H., Ambrizzi, T., Vera, C.S., Saulo, A.C., Nogues-Paegle, J., Zipser, E., Seth, A., Alves, L.M., 2012. Recent developments on the south american monsoon system. Int. J. Climatol. 32, 1–21. https://doi.org/10.1002/joc.2254.

McClintock, T.R., Chen, Y., Bundschuh, J., Oliver, J.T., Navoni, J., Olmos, V., Lepori, E.V., Ahsan, H., Parvez, F., 2012. Arsenic exposure in Latin America: biomarkers, risk assessments and related health effects. Sci. Total Environ. 429, 76–91. https://doi.org/10.1016/j.scitotenv.2011.08.051.

Miller, J.N., 1991. Basic statistical methods for analytical chemistry. Part 2. Calibration and regression methods. A review. Analyst 116, 3. https://doi.org/10.1039/an9911600003.

Ministerio de Bienes Nacionales, 2019. Infraestructura de datos geoespaciales (Chile).

Morales-Simfors, N., Bundschuh, J., Herath, I., Inguaggiato, C., Caselli, A.T., Tapia, J., Choquehuayta, F.E.A., Armienta, M.A., Ormachea, M., Joseph, E., López, D.L., 2020. Arsenic in Latin America: a critical overview on the geochemistry of arsenic originating from geothermal features and volcanic emissions for solving its environmental consequences. Sci. Total Environ. 716, 135564. https://doi.org/10.1016/j.scitotenv.2019.135564.

Moreno, T., Gibbons, W., 2007. The Geology of Chile. The Geological Society of London, London https://doi.org/10.1144/GOCH.

Mukherjee, A., Gupta, S., Coomar, P., Fryar, A.E., Guillot, S., Verma, S., Bhattacharya, P., Bundschuh, J., Charlet, L., 2019. Plate tectonics influence on geogenic arsenic cycling: from primary sources to global groundwater enrichment. Sci. Total Environ. 683, 793–807. https://doi.org/10.1016/j.scitotenv.2019.04.255.

Murray, J., Nordstrom, D.K., Dold, B., Romero Orué, M., Kirschbaum, A., 2019. Origin and geochemistry of arsenic in surface and groundwaters of Los Pozuelos basin, Puna region, Central Andes, Argentina. Sci. Total Environ. 697, 134085. https://doi.org/10.1016/j.scitotenv.2019.134085.

OSMF, 2019. Land polygons - OpenStreetMap [WWW document]. URL https://osmdata.openstreetmap.de/data/land-polygons.html.

Pincetti-Zúniga, G.P., Richards, L.A., Tun, Y.M., Aung, H.P., Swar, A.K., Reh, U.P.Hya, Khaing, T., Hlaing, M.M., Myint, T.A., Nwe, M.L., Polya, D.A., 2020. Major and trace (including arsenic) groundwater chemistry in central and southern Myanmar. Appl. Geochem. 115, 104535. https://doi.org/10.1016/j.apgeochem.2020.104535.

Pizarro, J., Vergara, P.M., Rodríguez, J.A., Valenzuela, A.M., 2010. Heavy metals in northern chilean rivers: spatial variation and temporal trends. J. Hazard. Mater. 181, 747–754. https://doi.org/10.1016/j.jhazmat.2010.05.076.

Polya, D.A., Lawson, M., 2015. Geogenic and anthropogenic arsenic hazards in groundwater and soils: distribution, nature, origin and human exposure routes. In: States, J.C. (Ed.), Arsenic: Exposure Sources, Health Risks and Mechanisms of Toxicity. John Wiley & Sons. ISBN: 978-1-118-51114-5, pp. 23–60.

Polya, D.A., Watts, M.J., 2017. Chapter 5: sampling and analysis for monitoring arsenic in drinking water. In: Bhattacharya, P., Polya, D.A., Jovanovic, D. (Eds.), Best Practice Guide on the Control of Arsenic in Drinking Water https://doi.org/10.2166/9781780404929_049.

Rámila, C.D.P., Leiva, E.D., Bonilla, C.A., Pastén, P.A., Pizarro, G.E., 2015. Boron accumulation in Puccinellia frigida, an extremely tolerant and promising species for boron phytoremediation. J. Geochem. Explor. 150, 25–34. https://doi.org/10.1016/j.gexplo.2014.12.020.

Ravenscroft, P., Brammer, H., Richards, K.S., 2009. Arsenic Pollution: A Global Synthesis. Wiley-Blackwell.

Rech, J.A., Currie, B.S., Shullenberger, E.D., Dunagan, S.P., Jordan, T.E., Blanco, N., Tomlinson, A.J., Rowe, H.D., Houston, J., 2010. Evidence for the development of the Andean rain shadow from a Neogene isotopic record in the Atacama Desert, Chile. Earth Planet. Sci. Lett. 292, 371–382. https://doi.org/10.1016/j.epsl.2010.02.004.

Richards, L.A., Magnone, D., Sovann, C., Kong, C., Uhlemann, S., Kuras, O., van Dongen, B.E., Ballentine, C.J., Polya, D.A., 2017. High resolution profile of inorganic aqueous geochemistry and key redox zones in an arsenic bearing aquifer in Cambodia. Sci. Total Environ. 590–591, 540–553. https://doi.org/10.1016/j.scitotenv.2017.02.217.

Risacher, F., Alonso, H., Salazar, C., 1999. Geoquímica de aguas en cuencas cerradas: I, II y II regiones. Chile [WWW document] . https://snia.mop.gob.cl/sad/CQA1921v4.pdf.

Risacher, F., Alonso, H., Salazar, C., 2003. The origin of brines and salts in chilean salars: a hydrochemical review. Earth Sci. Rev. 63, 249–293. https://doi.org/10.1016/S0012-8252(03)00037-0.

Risacher, F., Fritz, B., Hauser, A., 2011. Origin of components in chilean thermal waters. J. S. Am. Earth Sci. 31, 153–170. https://doi.org/10.1016/J.JSAMES.2010.07.002.

Rissmann, C., Leybourne, M., Benn, C., Christenson, B., 2015. The origin of solutes within the groundwaters of a high andean aquifer. Chem. Geol. 396, 164–181. https://doi.org/10.1016/j.chemgeo.2014.11.029.

Romero, L., Alonso, H., Campano, P., Fanfani, L., Cidu, R., Dadea, C., Keegan, T., Thornton, I., Farago, M., 2003. Arsenic enrichment in waters and sediments of the rio Loa (Second region, Chile). Appl. Geochem. 18, 1399–1416. https://doi.org/10.1016/S0883-2927(03)00059-3.

Sancha, A.M., O'Ryan, R., 2008. Managing hazardous pollutants in Chile: arsenic. Rev. Environ. Contam. Toxicol. 196, 123–146. https://doi.org/10.1007/978-0-387-78444-1_5.

Sarricolea, P., Meseguer Ruiz, Ó., Romero-Aravena, H., 2017. Precipitation trends in the Chilean norte grande and its relationship with climate change projections. Dialogo Andin. 41–50. https://doi.org/10.4067/S0719-26812017000300041.

SEA-Energia Andina, 2013. Evaluación Ambiental: Prospección Geotermal Colpitas. Antecedentes hidroquímicos e isotópicos de manatiales fríos, precipitaciones y escorrentías, Proyecto Geotérmico Colpitas.

SEA-ESSAT, 1999. Declaración de Impacto Ambiental: Mejoramiento de calidad de agua sistema de produccion Lluta Bajo. Sistema de Abatimiento de Manganeso y Fierro. [WWW document]. URL https://seia.sea.gob.cl/archivos/DIA/2013090201/DIA_2446_DOC_2128535999.pdf.

SEA-GHD, 2011. Declaración de Impacto Ambiental: Planta de Tratamiento de Agua Potable Recinto Pago de Gómez, Arica [WWW document]. URL https://seia.sea.gob.cl/documentos/documento.php?idDocumento=6217224.

SEA-SGA, 2010. Estudio de Impacto Ambiental: Planta de Manganeso Los Pumas [WWW document]. URL https://seia.sea.gob.cl/documentos/documento.php?idDocumento=5661949.

SEA-SRK Consulting, 2002. Declaración de Impacto Ambiental: Optimización del Proyecto Minero Choquelimpie [WWW document]. URL https://seia.sea.gob.cl/expediente/expedientesEvaluacion.php?id_expediente=5606&idExpediente=5606.

Sernageomin, 2003. Mapa geologico de chile: Version Digital. Publicacion Geologia Digital.
Servicio Nacional de Geología y Minería, 2012. Cartas Visviri y Villa Industrial - Región de Arica y Parinacota. Carta Geológica de Chile. Serie Geología Básica Escala 1:100.000.
Smedley, P.L., Kinniburgh, D.G., 2002. A review of the source, behaviour and distribution of arsenic in natural waters. Appl. Geochem. 17, 517–568. https://doi.org/10.1016/S0883-2927(02)00018-5.
SMI, 2008. Diagnóstico y diseño definitivo reparación Embalse Caritaya, Camarones.
Smith, A.H., Hopenhayn-Rich, C., Bates, M.N., Goeden, H.M., Hertz-Picciotto, I., Duggan, H.M., Wood, R., Kosnett, M.J., Smith, M.T., 1992. Cancer risks from arsenic in drinking water. Environ. Health Perspect. 97, 259–267. https://doi.org/10.1289/ehp.9297259.
Smith, A.H., Arroyo, A.P., Guha Mazumder, D.N., Kosnett, M.J., Hernandez, A.L., Beeris, M., Smith, M.M., Moore, L.E., 2000. Arsenic-induced skin lesions among atacameno people in northern Chile despite good nutrition and centuries of exposure. Environ. Health Perspect. 108, 617–620. https://doi.org/10.1289/ehp.00108617.
Smith, A.H., Marshall, G., Roh, T., Ferreccio, C., Liaw, J., Steinmaus, C., 2017. Lung, Bladder, and Kidney Cancer Mortality 40 Years After Arsenic Exposure Reduction. https://doi.org/10.1093/jnci/djx201.
Steinmaus, C.M., Ferreccio, C., Romo, J.A., Yuan, Y., Cortes, S., Marshall, G., Moore, L.E., Balmes, J.R., Liaw, J., Golden, T., Smith, A.H., 2013. Drinking water arsenic in northern Chile: high cancer risks 40 years after exposure cessation. Cancer Epidemiol. Biomark. Prev. 22, 623–630. https://doi.org/10.1158/1055-9965.EPI-12-1190.
Steinmaus, C., Ferreccio, C., Acevedo, J., Balmes, J.R., Liaw, J., Troncoso, P., Dauphiné, D.C., Nardone, A., Smith, A.H., 2016. High risks of lung disease associated with early-life and moderate lifetime arsenic exposure in northern Chile. Toxicol. Appl. Pharmacol. 313, 10–15. https://doi.org/10.1016/j.taap.2016.10.006.
Tapia, D., 2019. Región de Arica y Parinacota: Minería como oportunidad real de desarrollo | Revista Nueva Minería & Energía [WWW Document]. URLRev. Nueva Minería y Energía (accessed 9.21.20) https://www.nuevamineria.com/revista/region-de-arica-y-parinacota-mineria-como-oportunidad-real-de-desarrollo/.
Tapia, J., Davenport, J., Townley, B., Dorador, C., Schneider, B., Tolorza, V., von Tümpling, W., 2018. Sources, enrichment, and redistribution of As, Cd, Cu, Li, Mo, and Sb in the Northern Atacama Region, Chile: implications for arid watersheds affected by mining. J. Geochem. Explor. 185, 33–51. https://doi.org/10.1016/j.gexplo.2017.10.021.
Tapia, J., Murray, J., Ormachea, M., Tirado, N., Nordstrom, D.K., 2019. Origin, distribution, and geochemistry of arsenic in the Altiplano-Puna plateau of Argentina, Bolivia, Chile, and Perú. Sci. Total Environ. 678, 309–325. https://doi.org/10.1016/j.scitotenv.2019.04.084.
Tapia, J., Schneider, B., Inostroza, M., Álvarez-Amado, F., Luque, J.A., Aguilera, F., Parra, S., Bravo, M., 2021. Naturally elevated arsenic in the Altiplano-Puna, Chile and the link to recent (Mio-Pliocene to Quaternary) volcanic activity, high crustal thicknesses, and geological structures. J. S. Am. Earth Sci. 105, 102905. https://doi.org/10.1016/j.jsames.2020.102905.
Tassi, F., Aguilera, F., Darrah, T., Vaselli, O., Capaccioni, B., Poreda, R.J., Delgado Huertas, A., 2010. Fluid geochemistry of hydrothermal systems in the Arica-Parinacota, Tarapacá and Antofagasta regions (northern Chile). J. Volcanol. Geotherm. Res. 192, 1–15. https://doi.org/10.1016/j.jvolgeores.2010.02.006.
Todolí, J.L., Gras, L., Hernandis, V., Mora, J., 2002. Elemental matrix effects in ICP-AES. J. Anal. At. Spectrom. https://doi.org/10.1039/b009570m.
Torres, A., Acevedo, E., 2008. El Problema De Salinidad En Los Recursos Suelo Y Agua Que Afectan El Riego Y Cultivos En Los valles de Lluta y Azapa en el Norte de Chile. Idesia 26, 31–44. https://doi.org/10.4067/S0718-34292008000300004.
USGS, 2021. EarthExplorer [WWW document]. URL https://earthexplorer.usgs.gov/.
UTA, 2010. Cuenca de Camarones: Identificación y caracterización de fuentes que condicionan la calidad de las aguas superficiales: rol del embalse Caritaya [WWW Document]. URL http://icass.zteeo.com/gallery/2/1.31 UTA-DGA, 2010a. Apoyo Técnico para la mesa regional del agua en la región de Arica y Parinacota 2010.pdf.
Valenzuela, C., Campos, V.L., Yañez, J., Zaror, C.A., Mondaca, M.A., 2009. Isolation of Arsenite-Oxidizing Bacteria from Arsenic-Enriched Sediments from Camarones River, Northern Chile. Bull. Environ. Contam. Toxicol. 82, 593–596. https://doi.org/10.1007/s00128-009-9659-y.
Vega, M., Pardo, R., Barrado, E., Deb?n, L., Debán, L., 1998. Assessment of seasonal and polluting effects on the quality of river water by exploratory data analysis. Water Res. 32, 3581–3592. https://doi.org/10.1016/S0043-1354(98)00138-9.
Watts, M.J., O'Reilly, J., Marcilla, A.L., Shaw, R.A., Ward, N.I., 2010. Field based speciation of arsenic in UK and Argentinean water samples. Environ. Geochem. Health 32, 479–490. https://doi.org/10.1007/s10653-010-9321-y.
Webster, J.G., Nordstrom, D.K., 2003. Geothermal Arsenic. In: Welch, A.H., Stollenwerk, K.G. (Eds.), Arsenic in Ground Water. Springer, Boston, pp. 101–125 https://doi.org/10.1007/b101867.
WHO, 2017. Guidelines for Drinking-water Quality: Fourth Edition Incorporating the First Addendum. WHO Library Cataloguing-in-Publication Data, Geneva.
Williams, W.D., 1999. Salinisation: a major threat to water resources in the arid and semi-arid regions of the world. Lakes Reserv. Res. Manag. 4, 85–91. https://doi.org/10.1046/j.1440-1770.1999.00089.x.